EP04/06916

Europäisches Patentamt
European Patent Office
Office européen des brevets

Bescheinigung Certificate Attestation

Die angehefteten Unterlagen stimmen mit der ursprünglich eingereichten Fassung der auf dem nächsten Blatt bezeichneten europäischen Patentanmeldung überein.

The attached documents are exact copies of the European patent application described on the following page, as originally filed.

Les documents fixés à cette attestation sont conformes à la version initialement déposée de la demande de brevet européen spécifiée à la page suivante.

Patentanmeldung Nr. Patent application No. Demande de brevet n°

03014601.3

Der Präsident des Europäischen Patentamts;
Im Auftrag

For the President of the European Patent Office

Le Président de l'Office européen des brevets
p.o.

R C van Dijk

Europäisches Patentamt | European Patent Office | Office européen des brevets

Anmeldung Nr:
Application no.: 03014601.3
Demande no:

Anmeldetag:
Date of filing: 26.06.03
Date de dépôt:

Anmelder/Applicant(s)/Demandeur(s):

Max-Planck-Gesellschaft zur Förderung
der Wissenschaften e.V.
Hofgartenstrasse 8
80539 München
ALLEMAGNE

Bezeichnung der Erfindung/Title of the invention/Titre de l'invention:
(Falls die Bezeichnung der Erfindung nicht angegeben ist, siehe Beschreibung.
If no title is shown please refer to the description.
Si aucun titre n'est indiqué se referer à la description.)

Determination of voltage changes using a voltage-sensitive dye

In Anspruch genommene Priorität(en) / Priority(ies) claimed /Priorité(s) revendiquée(s)
Staat/Tag/Aktenzeichen/State/Date/File no./Pays/Date/Numéro de dépôt:

Internationale Patentklassifikation/International Patent Classification/
Classification internationale des brevets:

G01N33/48

Am Anmeldetag benannte Vertragstaaten/Contracting states designated at date of filing/Etats contractants désignées lors du dépôt:

AT BE BG CH CY CZ DE DK EE ES FI FR GB GR HU IE IT LU MC NL
PT RO SE SI SK TR LI

26. Juni 2003

WEICKMANN & WEICKMANN

Patentanwälte
European Patent Attorneys · European Trademark Attorneys

EPO - Munich
74
26. Juni 2003

DIPL.-ING. H. WEICKMANN (bis 31.1.01)
DIPL.-ING. F. A. WEICKMANN
DIPL.-CHEM. B. HUBER
DR.-ING. H. LISKA
DIPL.-PHYS. DR. J. PRECHTEL
DIPL.-CHEM. DR. B. BÖHM
DIPL.-CHEM. DR. W. WEISS
DIPL.-PHYS. DR. J. TIESMEYER
DIPL.-PHYS. DR. M. HERZOG
DIPL.-PHYS. B. RUTTENSPERGER
DIPL.-PHYS. DR.-ING. V. JORDAN
DIPL.-CHEM. DR. M. DEY
DIPL.-FORSTW. DR. J. LACHNIT

Unser Zeichen:
30928P EP/MDmh

Anmelder:
Max-Planck-Gesellschaft zur
Förderung der Wissenschaften e.V.
Hofgartenstraße 8

80539 München

Determination of voltage changes using a voltage-sensitive dye

---

Postfach 860 820, 81635 München, Deutschland, Tel. (089) 45563 0. Fax (089) 45563 999. email@weickmann.de

Determination of voltage changes using a voltage-sensitive dye

Description

The present invention relates to a method of determining voltage changes, e.g. in cell membranes, by means of a voltage-sensitive dye.

The recording of neuronal activity is an essential prerequisite to investigate the electric function of nerve cells, neuronal networks and the brain. Such applications basically require dyes exhibiting a great fluorescence change at small voltage changes. Numerous dyes have been developed to this end over the years (Loew, L.M.; Bonneville, G.W.; Surow, J., Biochemistry 1978, 17, 4065; Loew, L.M., Simpson, L.L., Biophys. J. 1981, 34, 353; (9) Fluhler, E., Burnham, V.G., Loew, L.M. Biochemistry 1985, 24, 5749; Grinvald, A., Hildesheim, R., Farber, I.C., Anglister, L. Biophys. J. 1982, 39, 301; Grinvald, A., Fine, A., Farber, I.C., Hildesheim, R. Biophys. J. 1983, 42, 195), especially the dyes di-4-ANEPBS and RH-421. Most popular are styrene-type hemicyanines where aniline as an electron donor is joined to pyridinium as an electron acceptor by one, two or three conjugated CC double bonds.

In conventional methods of determining voltage changes, particularly in the case of nerve cells, however, the problem is that voltage-dependent dyes typically indicate fluorescence changes of only a few percent per 100 mV membrane voltage change. Therefore, the signal-to-noise ratio is often very low due to an excitation in or including a highly efficient absorption range of the dye. Further, due to a strong phototoxicity of most photosensitive dyes only short measurement times are possible for a single cell.

An object of the present invention, therefore, was to provide a new process for an improved measurement of voltage changes overcoming the limitations of the prior art.

According to the invention this object is solved by a process for determining voltage changes by means of a voltage-sensitive dye, characterized in that the voltage-sensitive dye is irradiated with light having a wavelength, at which the dye has an absorption ≤ 20% of its absorption maximum and the fluorescence caused by irradiation with light is measured.

According to the invention changes in voltage, in particular, in transmembrane voltage, are determined using voltage-dependent dyes, which show a change in fluorescence depending on the voltage they experience. Usually lamps and filters or lasers are used for excitation. However, excitation can be effected by any light source. According to the invention excitation is effected at a wavelength or a wavelength band, at which absorption of the dye is ≤ 20%, preferably ≤ 10%, in particular, ≤ 5%, more preferably ≤ 3% and most preferably ≤ 2% of the absorption maximum. According to the invention no light is irradiated to the dye, which has a wavelength, at which the absorption of the dye is ≥ 20%, preferably ≥ 10%, in particular, ≥ 5%, more preferably ≥ 3% and most preferably ≥ 2% of its absorption maximum. Surprisingly, it has been found that in the case of such measurements at the spectral egde, especially at the red spectral edge of the excitation spectrum (i.e. at the edge shifted towards light having longer wavelength, related to the absorption maximum), the sensitivity of measurement is increased.

According to the invention, particularly, an increase or decrease of fluorescence is measured which can be observed in the case of the photosensitive dyes when radiated with light due to a change in voltage of the environment, e.g. a change of transmembrane voltage.

Specifically, the invention relates to a method of measuring voltage changes in cells such as nerve cells and in cell membranes.

According to the invention, a voltage-sensitive dye is used. Suitable dyes are described in literature (Loew, L.M., Bonneville, G.W., Surow, J.Biochemistry 1978, 17, 4065; Loew, L.M., Simpson, L.L. Biophys. J. 1981, 34, 353; Fluhler, E., Burnham, V.G., Loew, L.M., Biochemistry 1985, 24, 5749; Grinvald, A., Hildesheim, R., Farber,

I.C., Anglister, L. Biophys. J. 1982, 39, 301; Grinvald, A., Fine, A., Farber, I.C., Hildesheim, R. Biophys. J. 1983, 42, 195). Suitable fluorescent dyes, for example, are hemicyanines having a hydrophilic head group and a hydrophobic end region. The hydrophilic part usually comprises a sulfate group (negatively charged) and pyridine (positively charged), while the hydrophobic end is composed of aniline and two hydrocarbon groups. Thus, the dyes are amphiphilic and deposit in lipid membranes. In the case of these dyes the chromophore being a coherent electron system is formed by pyridine and aniline which are interconnected by alternating single and double bonds of hydrocarbons. Such dyes show an electrochromic response to membrane voltage changes, a solvatochromic effect, photoisomerism of CC double bonds and photorotamerism of CC single bonds. The electrochromic effect is due to the Stark effect. The solvatochromic effect leads to a movement of the dye in its surrounding solvent due to changes in the electric field, which also results in spectral changes.

According to the invention hemicyanine dyes having linearly anellated benzene rings are preferably used as they do not show solvatochromic effects during voltage changes and as they cannot isomerize or rotate (no CC single or CC double bonds). Preferred are those hemicyanine dyes with at least 3, in particular, at least 4, more preferred at least 5 and most preferred at least 6 and up to 20, more preferred up to 10 and most preferred up to 8 linearly anellated benzene rings. Preferred compounds have the formula

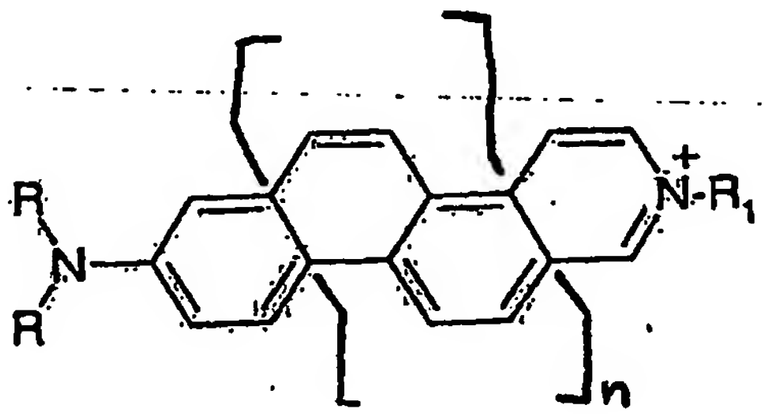

or

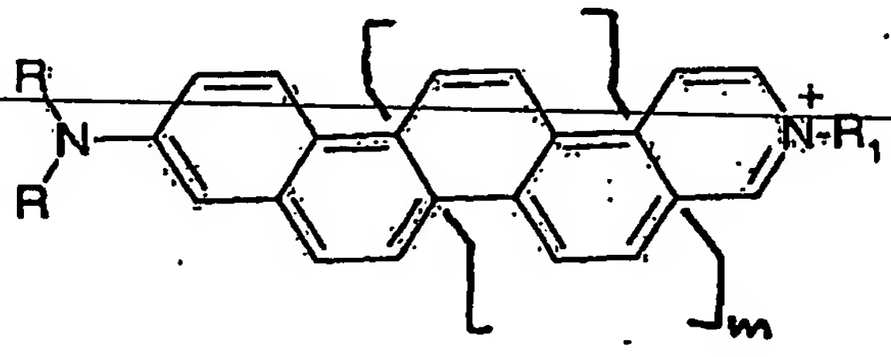

and more preferred compounds comprise the compounds ANNINE-4, ANNINE-5, ANNINE-6 and ANNINE-7 having the general formula

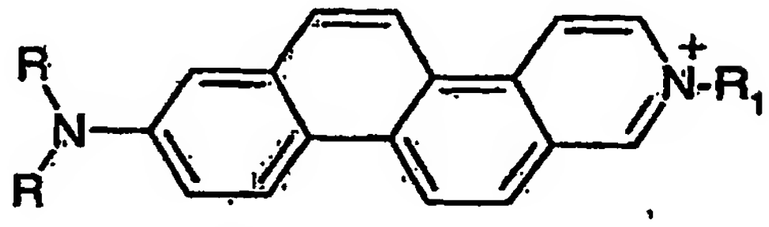

ANNINE-4

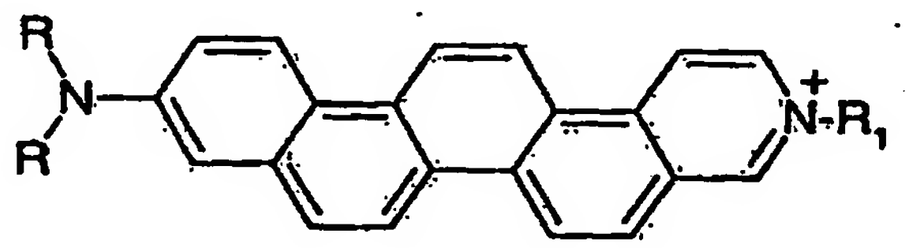

ANNINE-5

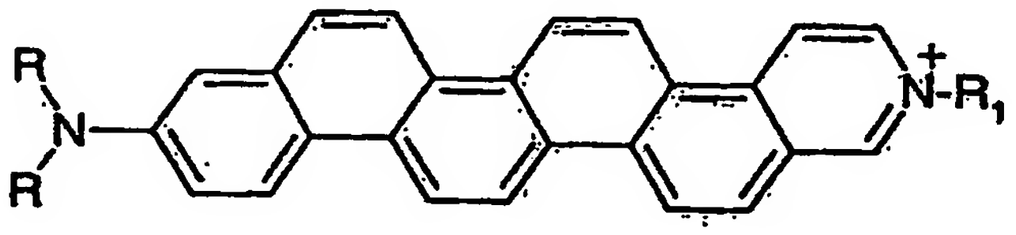

ANNINE-6

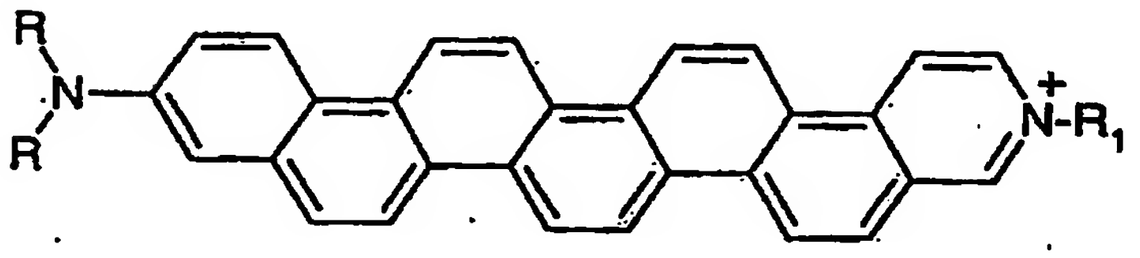

ANNINE-7

wherein each R independently is a hydrocarbon residue which can be linear or branched, saturated or mono- or polyunsatured and which has1-30, preferably 1-10 carbon atoms, and may be substituted with hydroxyl,

R^1 is a monovalent residue,

n is an integer from 1 to 9 and m is an integer from 0 to 8. Particularly, R^1 is an organic residue comprising 1 to 50, in particular, 1 to 30 C atoms and optionally heteroatoms, in particular, selected from N, S, O and P. While R^1 can be neutral, it is

preferably a negatively or positively charged residue. R^1 preferably is a hydrocarbon residue which can be linear or branched, saturated or mono- or polyunsatured and which has1-30, preferably 1-10 carbon atoms, e.g. methyl, ethyl, propyl, butyl, etc. Especially preferably R^1 is a residue R^2-SO_3^- ,wherein R^2 is a hydrocarbon group which can be linear or branched and either saturated or mono- or polyunsatured and which has 1-30, particularly 1-10 carbon atoms. In a further preferred embodiment R^1 is a positively charged residue such as R^2-$N^+(R)_3$, e.g. $(CH_2)_3N^+(CH_3)_3$, forming a dicationic dye. Such dicationic dyes show improved solubility in water up to total water solubility (without any need of additional organic solvents) while retaining voltage sensitivity. Especially preferably R is butyl residue and R^1 is a residue $(CH_2)_4SO_3^-$.

In particular, the dyes ANNINE-5, ANNINE-6, ANNINE-7 and ANNINE-8 show a pure electrochromic response to membrane voltage changes. This leads to a sensitivity increase at the red edge of the spectrum. Using narrowband excitation (laser) (e.g. < 40 nm width) at the very long-wavelength edge of the spectrum, sensitivities of up to 90% for100 mV can be achieved. The pure spectral shift caused by the Stark effect , which is not overlapped by other effects, e.g. solvatochromism, offers numerous advantages in practice. Sensitivity is increased and the spectra obtained are markedly easier to understand. Further, specifically ANNINE-6 and ANNINE- 7 show a very large intramolecular charge shift that leads to a strong spectral shift and so to the extremely high sensitivity.

The pure spectral shift ensures that the sensitivity increases sharply at the spectral edge. This means that the effective signal-to-noise ratio decreases much less than the absorption cross-section and the information obtained per absorption event strongly increases. Since phototoxicity is dependent on absorption, this also means that either the number of tests which can be carried out on a cell can be increased or the sensitivity of the tests can be enhanced. When increasing the excitation wavelength, a thermodynamical limit is nearly reached, at which no further sensitivity increase is achieved. In the case of ANNINE-6 and an excitation wavelength of 515 nm a sensitivity of +90% for -100 mV (or -45% for +100 mV) for dyes incorporated at the outer side of the membrane and +90% for +100 mV (or -45% for -100 mV) for

dyes incorporated inside the cells (as expected) could be achieved. This sensitivity is four times higher than the highest hitherto published value. Such high sensitivities also enable the detection of small (e.g. ≤ 10 mV, particulary ≤ 5 mV) and/or rapid (1 ms time resolution) voltage changes. This sensitivity range is not covered by existing high throughput screening methods. The increased relative changes furthermore reduce the dependency on instrumental shortcomings, e.g. variations of the illumination intensity.

In the case of the dye ANNINE-6 measurement is carried out preferably at wavelenths in the range of from 500 nm to 530 nm.

It has been found that sensitivity (i.e. the relative fluorescence change) at wavelengths which are closer to the absorption maximum (i.e. ranges having an absorption > 5%) is not so good as in the range according to the invention.

Another advantage of the ANNINE dyes preferably used according to the invention is their quick reaction, so measurements in the sub-microsecond range are possible.

As the mechanism of voltage sensitivity in ANNINEs is very simple, they show the same voltage sensitivity in cells so different as leech neurons and HER293 cells. Therefore, they can be used for all different cell types. This can also become important for calibration.

In hemicyanine dyes with anellated benzene rings there is no photorotamerism and no photoisomerism around CC double bonds and CC single bonds. Their solvatochromism in bulk solvents suggests an intramolecular charge shift that is distinctly larger than in homologous styryl type hemicyanines. They are simple and most efficient voltage sensitive probes of voltage transients in biological membranes. In addition the ANNINE dyes may be used as sensitive probes of polarity and local electrical fields in colloids and polymers. Strong nonlinear optical effects are also expected.

Finally, it is also to be noted that molecules are inefficiently excited by irradation at the edge of the absorption spectrum (i.e. at ≤ 5% of the absorption maximum). To achieve higher excitation the intensity of the light irradiation can be increased. In this way the signal-to-noise ratio can be adjusted. In this way a longer measurement time and/or reduced damage to the tested cell can be achieved by exciting few molecules.

In another preferred embodiment of the invention voltage-sensitive dye signals were obtained with two-photon excitation. Thereby the same total energy as in the case of the above-described one-photon method is provided by two photons, i.e. the wavelength of the photons in the case of two-photon excitation is twice as long. The same sensitivities could be achieved at the corresponding excitation wavelengths, which allows to combine the high-voltage sensitivity of the above-described method with the advantages of two-photon excitation. The extreme red excitation using two-photon excliation allows the use of the complete emission (fluorescence) spectrum, even if the corresponding excitation wavelength based on one-photon excitation were within the emission (fluorescence) range of the dye. Two-photon excitation especially offers the advantages of deep penetration into the tissue, low phototoxicity because absoprtion takes place only in the focus as well as low background fluorescence. Due to this the method can be performed even more reliably.

The invention is further illustrated by the enclosed Figures and the Examples given below.

Example 1

Synthesis of ANNINE dyes

The ANNINE dyes were assembled by combining four different donor moieties (D_1 – D_4) with two different acceptor moieties (A_1 – A_2) as illustrated in Fig. 2.

3-N,N-Dibutylaminobutyl benzoate (1)[20]**.** 1-Iodobutane (114.3 ml, 1 mol) was added to a mixture of 3-aminobenzoic acid (Fluka, Switzerland, 34.3 g, 250 mmol) in

250 ml DMF and K_2CO_3 (103.5 g, 750 mmol). The mixture was stirred at 100 °C overnight and distributed between EtOAc and water. The organic layer was washed with brine, dried (Na_2SO_4) and concentrated *in vacuo*. Pure **1** (64.9 g, 85 % yield, colourless oil) was obtained by distillation (bp 153 °C, 0,01 mbar).

3-N,N-Dibutylaminobenzyl alcohol (2). To a magnetically stirred mixture of $LiAlH_4$ (5.3 g; 140 mmol) in 200 ml of anhydrous diethyl ether was added dropwise a solution of **1** (74.1 g, 240 mmol) in 200 ml anhydrous diethyl ether. The mixture was stirred overnight, then quenched by addition of ice cold water, triturated with 40 % NaOH and the organic layer separated. The ether extract was washed with brine, dried (Na_2SO_4) and evaporated. Destillation provided **2** (oil, bp 105 -110 °C, 0.01 mbar, 91 % yield).

3-N,N-Dibutylaminobenzyl chloride (3). PCl_5 (46.0 g, 220 mmol) was added in portions to **2** (52.3 g, 220 mmol). The black viscous mixture was stirred at 100°C for 1 h and then at room temperature overnight. The reaction mixture was quenched with ice and diluted ammonia and extracted with ether. The extract was washed with brine, dried (Na_2SO_4) and the solvent was evaporated. Chromatography (SiO_2, EtOAc: heptane 18:5) provided pure **3** (oil, bp 95 °C, 0,01 mbar, yield 79 %).

3-N,N-Dibutylaminobenzyltriphenylphosphonium chloride (4). A solution of **3** (19.4 g, 152 mmol) and PPh_3 (40 g, 152 mmol) in 120 ml toluene was refluxed for 16 h at 110 °C. Upon cooling the white precipitate was collected, washed with Et_2O and dried for 24 h at 50°C *in vacuo* to yield pure **4** (mp 165 °C, yield 63 %).

1-Bromo-6-N,N-dibutylaminonaphthalene (5). The synthesis was performed similarly to that previously described for 6-bromo-2-N,N-dibutylaminonaphthalene[20]. A mixture of 6-amino-1-bromonaphthalene[21] (29.15 g, 131.2 mmol, obtained from 2-nitronaphthalene (Lancaster, U.K.), *via* 1-bromo-6-nitronaphthalene[21,22] and subsequent reduction), 1-iodobutane (52.5 ml, 492.2 mmol) and anhydrous K_2CO_3 (36.0 g, 260 mmol) was heated in 250 ml dry DMF at 130°C for 48 h. Upon cooling water was added and the mixture extracted with $CHCl_3$ several times. The organic

extracts were dried (Na_2SO_4) and the solvent evaporated. By chromatography (SiO_2, EtOAc: heptane 3:7) pure **5** (brown oil, yield 77 %) was obtained.

6-N,N-Dibutylamino-1-cyanonaphthalene (6)[23]. A mixture of **5** (3.3 g, 10 mmol) and CuCN (1.07 g, 12 mmol) and 10 ml dry pyridine were refluxed at 220 °C for 72 h. Upon cooling and evaporation of the solvent the compound **6** (yellow solid, mp 33°C, yield 78 %) was isolated by chromatography (SiO_2, EtOAc: heptane 3:7).

6-N,N-Dibutylaminonaphthalene-1-carboxylic acid (7). A solution of **6** (1.4 g, 5 mmol) and NaOH (0.3 g, 7.5 mmol) in 20 ml 1-pentanole was stirred at 170 °C for 72 h. Then the solvent was evaporated and the residue distributed between EtOAc and water and acidified with 1 N HCl to pH 6. The organic layer was separated and the water extracted twice. The combined organic layer was dried (Na_2SO_4) and evaporated to give **7** (yellow solid, mp 78 °C, quant.).

6-N,N-Dibutylamino-1-hydroxymethylnaphthalene (8)[24]**.** To a stirred and ice-cooled mixture of $LiAlH_4$ (0.6 g, 15.8 mmol) and dry diethylether (50 ml) a solution of **7** (5.6 g, 18.7 mmol) in 70 ml dry diethylether was added dropwise; then the cooling was removed and the mixture stirred overnight. After the addition of water the resulting precipitate was removed by filtration; then the organic layer was washed with brine and dried (Na_2SO_4) and the solvent was evaporated. The resulting compound **8** (oil, yield 90 %) still containing minor impurities was used for the next step. The direct synthesis of **8** starting from **5** via the lithiated intermediate and subsequent reaction with formaldehyde is also possible but less effective. **1-**

Bromomethyl-6-N,N-dibutylaminonaphthalene (9)[24]**.** To a solution of the alcohol 8 (14.5 g, 51 mmol) in 60 ml of toluene PBr_3 (2.4 ml, 26 mmol) was added under vigorous stirring. After the reaction mixture was stirred overnight, icy-cold water and then 10 % $NaHCO_3$ was added. The product was extracted with EtOAc, the organic layer washed with brine, dried (Na_2SO_4) and the solvent evaporated. After purification by column chromatography (SiO_2, EtOAc: heptane 1:4) 13.2g **9** (yellow oil, which solidifies in the freezer; yield 75 %) were obtained.

6-N,N-Dibutylaminonaphthyl-(1)-methyltriphenylphosphoniumbromid (10). A solution of **9** (12.7 g, 36.6 mmol) and PPh_3 (9.6 g, 36.6 mmol) in 40 ml was refluxed for 7 h. Upon cooling 450 ml diethylether were added and the precipitate washed with diethylether twice to give pure **10** (22 g, mp 185-188 °C, yield 99 %).

2-Methoxymethylbenzaldehyde (11). 1,2-Bis(hydroxymethyl)benzene (Lancaster, U.K.) was reacted to 2-methylmethoxybenzyl alcohol (1 equiv. NaH in THF, then MeI, oil, yield 50%); subsequent oxidation (MnO_2 in $CHCl_3$) resulted **11** (oil bp 52 ºC (0.012 mbar), yield 82%)[25].

7-N,N-Dibutylaminophenanthryl-(1)-methyltriphenylphosphoniumbromide (12) resp. **8-N,N-dibutyl-aminochrysenyl-(1)-methyltriphenylphosphoniumbromide (13).** 20 mMol of the phosphonium salt **4** resp. **10** and 20 mMol sodiummethoxide were dissolved in dry methanol and stirred at 60 ºC for 3 h. Then 20 mMol of the aldehyde **11** in MeOH were added dropwise and the solution was allowed to reflux overnight. After evaporation of the solvent the crude product was purified by chromatography (silicagel; EtOAc:heptane 1:5) ; the obtained alkenes E/Z-2-(3-N,N-dibutylamino-styryl)benzylmethylether **14a** (yield 50%) resp. E/Z-2-(6-N,N-dibutylamino-1-naphthyl)vinylbenzylmethylether **15a** (yield 61%) were cyclizysed as described below (20 h, solvent CH_2Cl_2) to the 7-N,N-dibutylamino-1-methoxy-methylphenanthrene **14** (yield 40%, oil) resp. 2-N,N-dibutylamino-7-methoxymethylchrysene **15** (yield 50%, m.p. 215 ºC). 10 mMol of the ethers **14** resp. **15** were stirred with 20 ml 62% HBr at 60 ºC for10 min. After neutralisation ($KHCO_3$) the crude products were extracted with $CHCl_3$ and purified by chromatography (silicagel; EtOAc:heptane 1:5) to receive 7-N,N-dibutylamino-1-bromomethylphenanthrene **16** (yield 53%,oil) resp. 2-N,N-dibutylamino-7-bromomethylchrysene **17** (yield 50%, m.p. 186 ºC (dec.)). Treatment of **16** resp.**17** with triphenylphosphine yielded the phosphonium salts **12** (yield 81%, m.p. 213-214 ºC) resp. **13** (yield 93%, mp 206 ºC).

5-Formylisoquinoline (18) was obtained from 5-bromoisoquinoline[26] in analogy to 4-

formylisoquinoline[27] (mp 116 °C[28], yield 55%).

E/Z-3-(3-N,N-Dibutylaminostyryl)-pyridine (19): 3.5 mMol of the phosphonium salt **4** was dissolved in dry MeOH, 190 mg (3.5 mMol) NaOMe was added and the mixture was allowed to reflux for 3 h; then 3.5 mMol of the 3-formylpyridine (Fluka) dissolved in MeOH was added; then the solution was refluxed overnight. The E/Z mixture was isolated by flash chromatography (silicagel, EtOAc:heptane 1:1). Yield 28%, yellow oil; EIMS *m/z* 308 (M^+), 265 (M^+-C_3H_7, $C_{21}H_{28}N_2$ requires 308.2).

E/Z-3-(6-N,N-Dibutylamino-1-naphthyl)-vinylpyridine (20): Same procedure as described for **19**, but using the phosphonium salt **10.** Yield 85%, yellow oil; EIMS *m/z* 358 (M^+), 315 (M^+-C_3H_7, $C_{25}H_{30}N_2$ requires 358.2).

E-5-(6-N,N-Dibutylamino-1-naphthyl)-vinylisoquinoline (21): Same procedure as described for **19**, but using the phosphonium salt **10** and aldehyde **18.** Yield 73%, yellow solid, mp 128-130 ºC (EtOAc); EIMS *m/z* 408 (M^+), 365 (M^+-C_3H_7, $C_{29}H_{28}N_2$ requires 408.3).

E/Z-5-(7-N,N-Dibutylamino-1-phenanthryl)-vinylisoquinoline (22): Same procedure as described for **19**, but using the phosphonium salt **12** and aldehyde **18**. Yield 82%, yellow solid, EIMS *m/z* 458 (M^+), 415 (M^+-C_3H_7, $C_{33}H_{34}N_2$ requires 458.3).

E/Z-5-(8-N,N-Dibutylamino-1-chrysenyl)-vinylisoquinoline (23): Same procedure as described for **19**, but using the phosphonium salt **13** and aldehyde **18**. Yield 80%, yellow solid; FABMS *m/z* 509.3 (M+1, $C_{37}H_{36}N_2$ requires 508.3).

Cyclisation of the alkenes 19-23[29]: A $5 \cdot 10^{-3}$ molar solution of the corresponding E-or E/Z-alkene was irradiated (45 min-40 h, duran glass, room temperature, CH_2Cl_2, unless stated otherwise) by a Hg high pressure lamp (TQ 150, Heraeus-Noblelight, Germany); after evaporation of the solvent the cyclisation products **24-26** were isolated by flash chromatography (EtOAc:heptane 1:1);crude **27** and **28** were obtained by precipitation from $CHCl_3$/MeOH and used for the final step without further

purification.

7-N,N-Dibutylamino-2-azaphenanthrene (24): yield 48%, 45 min irradiation (quartz glass, -30 ºC, 2-methyltetrahydrofuran), yellow oil; FABMS *m/z* 307.2 (M+1, $C_{21}H_{26}N_2$ requires 306.2).

8-N,N-Dibutylamino-2-azachrysene (25): yield 22%, 45 min irradiation (quartz glass, 0 ºC, cyclohexane), pale yellow solid, m.p.213 ºC (EtOAc); EIMS *m/z* 356 (M^+), 313 (M^+-C_3H_7, $C_{25}H_{28}N_2$ requires 356.2).

10-N,N-Dibutylamino-3-azapicene (26): yield 25%, 40 h irradiation (cyclohexane), pale yellow solid (EtOAc), still containing minor impurities; FABMS *m/z* 407.2 (M+1, $C_{29}H_{30}N_2$ requires 406.2).

11-N,N-Dibutylaminobenzo[m]-3-azapicene (27): yield 40% (crude product), 15 h irradiation; EIMS *m/z* 456 (M^+), 413 (M^+-C_3H_7, $C_{33}H_{32}N_2$ requires 456.3).

12-N,N-Dibutylaminonaphtho[5,6-m]-3-azapicene (28): yield 46% (crude product), 15 h irradiation; EIMS *m/z* 506 (M^+), 463 (M^+- C_3H_7, $C_{37}H_{34}N_2$ requires 506.3).

ANNINES 3-7: A mixture of 2 mMol of **24-28** and 5.4 g (40 mMol) 1,4-butane sultone was stirred at 120 ºC for 4h [20]. The resulting precipitate is collected, washed with ether and purified by flash chromatography (silica gel, MeOH or CH_2Cl_2:MeOH:H_2O 50:20:4 and Sephadex LH 20 (Pharmacia), MeOH) and recrystallised.

ANNINE-3: yield 24%, yellow solid m.p. >300 ºC(MeOH/heptane); FABMS *m/z* 443.2 (M+1, $C_{25}H_{34}N_2O_3S$ requires 442.2).

ANNINE-4: yield 35%, yellow solid m.p. >300 ºC(MeOH); FABMS *m/z* 493.5 (M+1, $C_{29}H_{36}N_2O_3S$ requires 492.2).

ANNINE-5: yield 40%, red-orange solid m.p. >300 ºC(MeOH); FABMS *m/z* 543.3

(M+1, $C_{33}H_{38}N_2O_3S$ requires 542.3).

ANNINE-6: yield 21 %, red-orange solid m.p. >300 ºC(MeOH); FABMS *m/z* 593.4 (M+1, $C_{37}H_{40}N_2O_3S$ requires 592.3).

ANNINE-7: yield 10 %, red solid m.p. >300 ºC(MeOH); FABMS *m/z* 643.5 (M+1, $C_{41}H_{42}N_2O_3S$ requires 642.3).

The structure of all dyes and intermediates was confirmed by mass spectroscopy and proton NMR.

The triphenylphosphonium salt D_1 was obtained in four steps from 3-aminobenzoic acid via 3-N,N-dibutylaminobutyl benzoate (1-iodobutane and K_2CO_3)[20], 3-N,N-dibutylaminobenzyl alcohol ($LiAlH_4$), 3-N,N-butylaminobenzyl chloride (with PCl_5) and subsequent treatment with PPh_3. This method is superior to the synthesis using 3-aminobenzaldehyde dimethyl acetal as a starting material[18]. For the synthesis of D_2 we brominated 2-nitronaphthalene; the resulting 1-bromo-6-nitronaphthalene[21,22] was reduced to 6-amino-1-bromonaphthalene ($SnCl_2$,HCl). Alklyation with 1-iodobutane leads to 1-bromo-6-N,N-dibutylaminonaphthalene[20]. Via 6-N,N-dibutylamino-1-cyanonaphthalene[23] (CuCN) and 6-N,N-dibutylaminonaphthalene-1-carboxylic acid (NaOH) we obtained by reduction ($LiAlH_4$) 6-N,N-dibutylamino-1-hydroxymethylnaphthalene[24]. (A direct synthesis starting from 1-bromo-6-N,N-dibutylaminonaphthalene via the lithiated intermediate and subsequent reaction with formaldehyde was less effective.) After bromination (PBr_3)[24] of the alcohol, a treatment with PPh_3 resulted in D_2.

To obtain D_3 we joined D_1 to 2-methoxymethylbenzaldehyde[25] by a Wittig reaction. Photocyclization of the alkenes E/Z-2-(3-N,N-dibutylamino-styryl)benzylmethylether produced 7-N,N-dibutylamino-1-methoxymethylphenanthrene, By ether cleavage we obtained 7-N,N-dibutylamino-1-bromomethylphenanthrene and with triphenylphosphine the product D_3. Starting from D_2 the same reaction sequence was performed to obtain D_4.

The acceptor moiety A_1 was commercially available. A_2 was obtained from 5-bromoisoquinoline[26] (BuLi, then DMF)[27,28]. Proper donor and acceptor moieties were chosen for Wittig reactions and subsequent photocyclization[29] to build up the scaffold of the ANNINES. So for example D_3 and A_2 were used for the formation of the six anellated rings of ANNINE-6. The last synthetic step was the reaction with 1,4-butane sultone.

References of Example 1:

(20) Hassner, A.; Birnbaum, D.; Loew, L. M. *J. Org. Chem.* **1984**, 49, 2546.

(21) v. Braun, J.; Hahn, E.; Seemann, J. *Chem. Ber.* **1922**, 55, 1687.

(22) Fieser, L. F.; Riegel, B. *J. Am. Chem. Soc.* **1937**, 59, 2561.

(23) Newman, M. S. *J. Am. Chem. Soc.* **1937**, 59, 2472.

(24) Szmuszkovicz, J.; Bergmann, E. D. *J. Am. Chem. Soc.* **1953**, 75, 353.

(25) Kirmse, W.; Kund, K. *J. Am. Chem. Soc.* **1989**, 111, 1465.

(26) Osborn, A. R.; Schofield, L. N. *J. Chem. Soc.* **1956**, 4191.

(2) Sainsbury, M.; Brown, D. W.; Dyke, S. F.; Clipperton, R. D. J.; Tonkyn, W. R. *Tetrahedron* **1970**, 26, 2239.

(28) Rodionov, V. M.; Alekseeva E. N.; Vleduts G. *J. Gen. Chem. USSR* **1957**, 27, 809.

(29) Muszkat, K. A. *Top. Curr. Chem.* **1980**, 88, 91.

Example 2

Absorption and fluorescence spectra

Solutions. We studied the absorption and fluorescence spectra in 17 solvents of increasing polarity: chloroform, decanol, benzyl alcohol, dichloromethane, octanol, cyclohexanol, hexanol, pentanol, cyclopentanol, butanol, propanol, ethylene glycol, dimethylformamide, acetone, ethanol, acetonitrile and methanol. Solvents of highest available purity were used (Merck, Darmstadt and Sigma, Taufkirchen, Germany). Stock solutions were made from methanol and chloroform at a volume ratio of 1:2 at a concentration of 1 mM for ANNINE-3, ANNINE-4 and ANNINE-5, and due to lower solubility 200 µM for ANNINE-6 and ANNINE-7. These stock solutions were diluted

by the different solvents to a final concentration 5µM, with the exception of ANNINE-7 in pentanol, butanol, acetone and acetonitrile where a concentration of 1µM was used.

Spectra. Absorption spectra were measured with a Varian Cary 3E spectrometer (Varian, Mulgrave, Victoria, Australia) at room temperature. Emission spectra were measured with a SLM Aminco 8100 fluorescence spectrometer that was adapted to the long wavelength region with a Spectra Pro-275 monochromator from Acton Research (Acton, MA, USA) containing appropriate gratings for the wavelength region up to 1200 nm and an avalanche photodiode as a detector (Polytec, Waldbronn, Germany). The spectrometer was calibrated with a 45 Watt quartz-halogen tungsten coiled filament lamp (OL 245M, Optronic Laboratories, Orlando, USA) as a standard of spectral irradiance. Calibration and measurement of the spectra were performed under magic angle conditions[30]. For ANNINE-3 the excitation bandwidth was 8 nm and the emission bandwidth was 18 nm. For ANNINE-4, ANNINE-5, ANNINE-6 and ANNINE-7 we used an excitation bandwidth of 16 nm and an emission bandwidth of 18 nm.

Evaluation of maxima: The maxima of the absorption spectra were automatically calculated by the Varian Cary software. For evaluation of the fluorescence maxima we fitted a log normal curve to each spectrum[31] according to Eq. 1 with an amplitude $F_{\bar{\nu}}^{MAX}$, a spectral maximum $\nu^{\bar{M}AX}$, a spectral width W and a spectral asymmetry b, excluding the contribution of the S_0/S_2 transition.

$$F_{\bar{\nu}}(\bar{\nu}) = F_{\bar{\nu}}^{MAX} \exp\left\{-\frac{\ln^2\left[1+2b\left(\bar{\nu}-\nu^{\bar{M}AX}\right)/W\right]}{b^2/\ln 2}\right\} \qquad (1)$$

The maximum was taken from the fit. For those solvents, where the second order Rayleigh scattering peak of the excitation light appeared on the flank of the spectrum, only the region of the maximum was used for evaluation.

Solvatochromism. The wavenumbers $\bar{\nu}_{abs}$ and $\bar{\nu}_{em}$ of the maxima of absorption and emission of the five hemicyanine dyes ANNINE-3 to ANNINE-7 in 17 solvents are plotted in Figure 3. The solvents are characterized by the polarity function

$F_1(\varepsilon, n)$ defined by Eq. 2[32] that depends on the static relative dielectric constant ε, the refractive index n of the solvent and an intramolecular dielectric constant ε_i.

$$F_1(\varepsilon, n) = \frac{1}{\varepsilon_i} \cdot \left(\frac{\varepsilon_i - n^2}{\varepsilon_i + 2n^2} - \frac{\varepsilon_i - \varepsilon}{\varepsilon_i + 2\varepsilon} \right) \qquad (2)$$

The values of $F_1(\varepsilon, n)$ with $\varepsilon_i = 2$ are for chloroform 0.1120, decanol 0.1623, benzyl alcohol 0.1697, dichloromethane 0.1722, octanol 0.1779, cyclohexanol 0.1915, hexanol 0.1971, pentanol 0.2011, cyclopentanol 0.2016, butanol 0.2136, propanol 0.2223, ethylene glycol 0.2272, dimethylformamide 0.2273, acetone 0.2294, ethanol 0.2342, acetonitrile 0.2479 and methanol 0.2497.

With all dyes there is a common trend for the maxima of absorption and fluorescence: increasing polarity shifts the absorption spectra to the blue and the emission spectra to the red. For each dye that divergent solvatochromism is rather symmetrical over the whole range of accessible polarity. I.e. it seems that the solvatochromism can be assigned to an increasing Stokes shift $\bar{\nu}_{abs} - \bar{\nu}_{em}$ with an invariant average $(\bar{\nu}_{abs} + \bar{\nu}_{em})/2$. I

Solvatochromism. From the experimental wavenumbers of absorption and emission in Fig. 3 we evaluate the averages $(\bar{\nu}_{ex} + \bar{\nu}_{em})/2$ and differences $(\bar{\nu}_{ex} - \bar{\nu}_{em})/2$ and plot them versus $F_1(E,n)$. As shown in Figs. 4a and 4b, the values of $(\bar{\nu}_{ex} + \bar{\nu}_{em})/2$ vary only by a few percent over the whole range of polarity, whereas the values of $(\bar{\nu}_{ex} - \bar{\nu}_{em})/2$ increase rather linearly.

Electrochromism. When a dye with an intramolecular charge displacement δ_{EG} is placed in an external electrical field, its absorption and emission band are shifted by a linear molecular Stark effect. In a biological membrane, the change of the electrical field is given by the change of membrane voltage ΔV_M and by the membrane thickness d_M .

We plot the expected electrochromic shift $\Delta\nu^{-}_{electro}$ in a membrane of thickness $d_M = 4\,nm$ and a voltage change $\Delta V_M = 100\,mV$ versus the solvatochromic sensitivity $\Delta\nu^{-}_{solv}$ in Fig. 6 for three different radii $a = 5, 7, 9\ A$ assuming a perfect orientation $\cos = 1$.

The experimental solvatochromic sensitivities $\Delta\nu^{-}_{solv}$ of the ANNINE dyes are marked by vertical lines in Fig. 6. The experimental electrochromic shifts of ANNINE-5 and ANNINE-6 in a neuron membrane are indicated by dots.[19] The electrical response in the neuron are in a range predicted by solvatochromism. Yet, the increase of electrochromism from ANNINE-5 to ANNINE-6 is stronger than expected for constant orientation $\cos\vartheta$ in the membrane and constant effective radius a in bulk solvents.

Example 3:

The voltage sensitivity of the anellated hemicyanines ANNINE-6 and ANNINE-5 and , also of BNBIQ, di-4-ANEPBS and RH-421 (was investigated). Twodimensional fluorescence spectra of excitation and emission are measured in leech neurons at defined membrane voltages. The voltage induced changes of fluorescence are parametrized in terms of changes of spectral parameters. ~~We find that the~~ ANNINE dyes are far more voltage sensitive than the classical styryl dyes and ~~that~~ their sensitivity can be assigned almost completely to an identical spectral shift of excitation and emission that is caused by a molecular Stark effect.

Dyes. The styryl dye RH-421 [11] was obtained from Molecular Probes (Eugene, OR, USA). The styryl dye di-4-ANEPBS [9] and the biaryl dye BNBIQ [22] were synthetized by Gerd Hübener. The synthesis of the dyes ANNINE-5 and ANNINE-6 is described above.

Neurons. Ganglia of the leech *Hirudo medicinalis* (Moser, Schorndorf, Germany) were dissected and pinned on a Sylgard coated dish in Leibowitz-15 medium (L-5520, Sigma, Deisenhofen) with 5 mg/ml glucose, 0.3 mg/ml glutamine and 3 µg/ml gentamycin sulfate (G-3632, Sigma) [24]. After opening the tissue capsules the ganglia were incubated in dispase/collagenase (Boehringer, Mannheim, 2 mg/ml L-15 medium) for 1 hour at room temperature. Retzius cells (soma diameter 60 – 90 µm) were dissociated by aspiration into a firepolished micropipette and washed with Leibowitz-15 medium [24]. The cells were seeded on an uncoated glass cover slip in a silicone chamber (Flexiperm-mikro 12, Vivascience AG, Hannover, Germany) with Leibowitz-

15 medium and 2.5 % fetal bovine serum (10106, Gibco, Eggenstein) and kept for one or two days at 20°C.

Staining. The dyes were solubilized in Leibowitz-15 medium with sodium cholate (Sigma, St. Luise, USA) [25]. We used 4.3 mM RH-421 with 10 mM cholate, 4.3 mM di-4-ANEPBS with 10mM cholate, 10 mM BNBIQ with 10 mM cholate, 1 mM ANNINE-5 with 23 mM cholate and 1 mM ANNINE-6 with 25 mM cholate. After centrifugation, the staining solutions were added to the culture chambers with the neurons at a volume ratio of 1:1000 30 min before patching. The solubility of the dyes in water decreases in the series RH-421, di4-ANEPBS, BNBIQ, ANNINE-5 and ANNINE-6. In correspondence, the fluorescence intensity of cells stained with RH-421 and di-4-ANEPBS dropped after exchanging the medium by a dye-free solution due to desorption from the cells, whereas the intensity with ANNINE-5 and ANNINE-6 remained constant for at least 1.5 h. With respect to bleaching and phototoxicity, we did not observe significant differences under comparable conditions of staining and illumination.

Electrophysiology. Patch pipettes with a tip diameter of 5 - 10 µm were made from micro haematocrite tubes (Assistent, Karl Hecht, Sondheim/Rhön, Germany) using an all-purpose puller (DMZ-Universal Puller, Zeitz-Instrumente, Augsburg, Germany). They were filled with 140 mM KCl, 1.5 mM $MgCl_2$, 10 mM Hepes and 10 mM EGTA, pH 7.3. The resistance of the pipettes was around 0.4 MΩ. The pipettes with Ag/AgCl electrodes were connected to a single electrode patch-clamp amplifier (SEC-10L, npi, Tamm, Germany). The patching of Retzius cells lead to a seal resistance of about 500 MΩ. Whole cell contact [26] was achieved by breaking the membrane by

suction using a water-jet vacuum pump. The bath was held on ground potential with a Ag/AgCl electrode. We kept the cells at an intracellular voltage of $V_M = -40mV$. The fluorescence spectra were measured at a hyperpolarized voltage of $V_M = -70mV$ and a depolarized voltage of about $V_M = 10mV$.

Optical setup. The spectrometer is sketched in Fig. 2. It is built on the basis of an inverted microscope (Axiovert 35, Zeiss, Oberkochen, Germany) with a high aperture oil immersion objective (Neofluar 100x/1,3 oil). The light of a 75 W Xenon short arc lamp (Ushio, Hyogo, Japan) is spectrally resolved (resolution 16 nm) by a grating monochromator (J&M, Aalen, Germany). It is fed into the microscope with an optical multimode fibre (diameter 1.2 mm) and a broadening optics (J&M). Nerve cell are illuminated through a dichroic mirror (AHF Analysentechnik, Tübingen, Germany) with a splitting wavelength of 520 nm for RH-421, di-4-ANEPPS, BNBIQ and ANNINE-6 and of 460 nm for ANNINE-5. The illumination is controlled by a shutter and a luminous field diaphragm. The light emitted by the stained cell is collected by the objective. It passes through the dichroic mirror and a long pass filter (AHF Analysentechnik, Tübingen) with cutoff at 520 nm for RH-421, di-4-ANEPBS, BNBIQ and ANNINE-6 and at 470 nm for ANNINE-5 and is guided by an optical fibre (0.6 mm) to a diode array spectrometer (J&M) with a spectral range from 307 nm to 1135 nm at a resolution of 3.1 nm.

Calibrated fluorescence spectra. In order to derive molecular parameters from the experimental data, the twodimensional spectra of excitation and emission were calibrated. The number of excitations per unit time in a membrane area A_{mem} with n_{dye}

molecules per unit area is $A_{mem}n_{dye}\varepsilon(\lambda_{ex})I_{\lambda}^{ill}(\lambda_{ex})\Delta\lambda_{ex}$ with the molecular cross section of absorption $\varepsilon(\lambda_{ex})$ and the quantum intensity of illumination per wavelength interval $I_{\lambda}^{ill}(\lambda_{ex})$ at a bandwidth $\Delta\lambda_{ex}$. The number of detected quanta per unit time $P(\lambda_{ex},\lambda_{em})$ is given by Eq. 1 with the quantum yield Φ_{em}, the normalized quantum spectrum of fluorescence per wavelength interval $f_{\lambda}(\lambda_{em})$ and the efficiency $T^{rec}(\lambda_{em})$ and bandwidth $\Delta\lambda_{em}$ of the recording system.

$$P(\lambda_{ex},\lambda_{em}) = A_{mem}n_{dye}\, I_{\lambda}^{ill}(\lambda_{ex})\,\Delta\lambda_{ex}\varepsilon(\lambda_{ex})\,\Phi_{em}f_{\lambda}(\lambda_{em})T^{rec}(\lambda_{em})\,\Delta\lambda_{em} \qquad (1)$$

We obtain a twodimensional fluorescence spectrum that is defined by molecular parameters when we divide Eq. 1 by the number of dye molecules $A_{mem}n_{dye}$ and by the spectra and bandwidths of illumination $I_{\lambda}^{ill}(\lambda_{ex})\Delta\lambda_{ex}$ and recording $T^{rec}(\lambda_{em})\Delta\lambda_{em}$. The resulting fluorescence spectrum of excitation and emission per unit wavenumber of emission $F_{\bar{\nu}}(\bar{\nu}_{ex},\bar{\nu}_{em}) = \varepsilon(\bar{\nu}_{ex})\,\Phi_{em}f_{\bar{\nu}}(\bar{\nu}_{em})$ is given by Eq. 2, considering the relations $f_{\bar{\nu}}(\bar{\nu}_{em}) = \lambda_{em}^2 f_{\lambda}(\lambda_{em})$ and $\varepsilon(\bar{\nu}_{ex}) = \varepsilon(\lambda_{ex})$.

$$F_{\bar{\nu}}(\bar{\nu}_{ex},\bar{\nu}_{em}) = \frac{\lambda_{em}^2}{A_{mem}n_{dye}I_{\lambda}^{ill}(\lambda_{ex})\Delta\lambda_{ex}T^{rec}(\lambda_{em})\Delta\lambda_{em}}P(\lambda_{ex},\lambda_{em}) \qquad (2)$$

$T^{rec}(\lambda_{em})\Delta\lambda_{em}$ is obtained up to an arbitrary factor by calibrating the recording system (objective, dichroic mirror, long pass filter, 0.6 mm fibre optics, monochromator and diode array). We place a standard lamp (OL245M, Optronic Laboratories, Orlando, USA) with a known quantum spectrum $I_{\lambda}^{cal}(\lambda)$ on the microscope and measure the response $P^{cal}(\lambda) = I_{\lambda}^{cal}(\lambda)T^{rec}(\lambda_{em})\Delta\lambda_{em}$ of the photodiode array. We probe the

illumination (Xe lamp, monochromator, optical fibre, broadening optics, dichroic mirror and objective) with a calibrated detector of efficiency $T^{cal}(\lambda)$ and bandwidth $\Delta\lambda$. For that purpose we use part of our recording system - the 0.6 nm optical fiber with monochromator and diode array – that is again calibrated by illuminating the fiber end with the standard lamp. With the fiber end on the microscope, we measure $P^{ill}(\lambda)=I_{\lambda}^{ill}(\lambda_{ex}^{nom},\lambda)T^{cal}(\lambda)\Delta\lambda$ for each λ_{ex}^{nom} set at the monochromator. The resulting illumination spectra $I_{\lambda}^{ill}(\lambda_{ex}^{nom},\lambda)$ are fitted with Gaussians with a maximum defining the excitation wavelenth λ_{ex} and an integral that represents the intensity $I_{\lambda}^{ill}(\lambda_{ex})\Delta\lambda_{ex}$ up to a constant factor.

Protocol. The measurements were started 30 min after staining. Under voltage clamp, the voltage sensitive fluorescence is investigated with the following protocol: (1) opening of the shutter, (2) selection of an excitation wavelength λ_{ex}, (3) after a delay of 100 ms hyperpolarization of the cell to $V_M=-70mV$, (4) recording of a complete emission spectrum in a range of $\lambda_{em}=510-833nm$ for RH-421, di-4-ANEPBS, BNBIQ and ANNINE-6 and $\lambda_{em}=460-833nm$ for ANNINE-5 with an integration time of 200 *ms*, (5) after a delay of 100 ms depolarization to about $V_M=10mV$, (6) recording of two complete emission spectra, (7) after a delay of 100 ms hyperpolarization to $V_M=-70mV$, (8) recording of another complete emission spectrum, (9) closing of the shutter. The steps (2)-(8) are repeated for various wavelengths of excitation in the range $\lambda_{ex}=360-510nm$ for RH-421, di-4-ANEPBS, BNBIQ and ANNINE-6 and $\lambda_{ex}=360-460nm$ for ANNINE-5 at a stepwidth of 5 *nm*. At each excitation wavelength the two spectra of the hyperpolarized cell are averaged as

well as the two spectra of the depolarized cell to obtain the spectra $P(\lambda_{ex},\lambda_{em})$ at the two voltages. The twodimensional fluorescence spectra $F_{\bar{\nu}}(\bar{\nu}_{ex},\bar{\nu}_{em})$ are computed according to Eq. 2 up to a constant factor using the spectra $I_{\lambda}^{III}(\lambda_{ex})\Delta\lambda_{ex}$ and $T^{rec}(\lambda_{em})\Delta\lambda_{em}$ given by calibration. At the hyperpolarized voltage the spectrum is scaled to its maximum as $F_{\bar{\nu}}^{hyp}/F_{\bar{\nu}}^{hyp,MAX}$. At the depolarized voltage the spectrum is scaled by the same factor as $F_{\bar{\nu}}^{dep}/F_{\bar{\nu}}^{hyp,MAX}$.

2D spectra. The relative fluorescence spectra per wavenumber interval of emission $F_{\bar{\nu}}(\bar{\nu}_{ex},\bar{\nu}_{em})/F_{\bar{\nu}}^{MAX}$ in Retzius neurons at a voltage $V_M = -70mV$ are plotted in the left column of Fig. 8 for RH-421, di4-ANEPBS, BNBIQ and ANNINE-5 and ANNINE-6. They are limited at the red end of excitation and the blue end of emission by the dichroic mirror of the microspectrometer. The maxima reflect the position of the upward and downward vibroelectronic transition between the S_0 and S_1 states of the dyes. They are shifted to higher wavenumbers of excitation and emission in the homologous series RH-421, di4-ANEPBS, BNBIQ and ANNINE-5 and also in ANNINE-6. With respect to excitation, a second band appears in the ANNINEs at high wavenumbers due to the S_0/S_2 transition.

1D spectra. In order to study the interdependence of excitation and emission, we consider mission spectra per wavenumber of emission $F_{\bar{\nu}}(\bar{\nu}_{em})$ at various wavenumbers of excitation $\bar{\nu}_{ex}$ and excitation spectra $F_{\bar{\nu}}(\bar{\nu}_{ex})$ per wavenumber of emission for

various wavenumbers of emission $\bar{\nu}_{em}$ in the twodimensional spectra. These onedimensional spectra are fitted by lognormal functions [27] according to Eq. 3 with an amplitude $F_{\bar{\nu}}^{MAX}$, a spectral maximum $\bar{\nu}^{MAX}$, a spectral width W and a spectral asymmetry b, excluding the contribution of the S_0/S_2 transition.

$$\frac{F_{\bar{\nu}}(\bar{\nu})}{F_{\bar{\nu}}^{MAX}} = \exp\left\{-\frac{\ln^2\left[1+2b\left(\bar{\nu}-\bar{\nu}^{MAX}\right)/W\right]}{b^2/\ln 2}\right\} \qquad (3)$$

Fig. 9 shows the parameters of the emission spectra $\bar{\nu}_{em}^{MAX}$, W_{em} and b_{em} as a function of the excitation wavenumber $\bar{\nu}_{ex}$ and the parameters of the excitation spectra $\bar{\nu}_{ex}^{MAX}$, W_{ex} and b_{ex} as a function of the emission wavenumber $\bar{\nu}_{em}$. The maximum of excitation is shifted to the blue at high wavenumbers of emission, and the maximum of emission is shifted to the blue for higher wavennumbers of excitation. Such effects are expected for hemicyanine dyes when the solvent shell is incompletely relaxed in the excited state [16]. However, these shifts of the spectral maxima as well as all other changes of spectral width and spectral asymmetry displayed in Fig. 9 are rather small compared with the width of the spectra and the difference of excitation and emission maxima. Considering these observations with the onedimensional spectra, we use in the following evaluation of the twodimensional spectra the approximation that excitation and emission processes are independent of each other.

Fit of 2D spectra. In order to attain awell defined parametrization of the fluorescence spectra, we fit the normalized 2D spectra $F_{\bar{\nu}}(\bar{\nu}_{ex},\bar{\nu}_{em})/F_{\bar{\nu}}^{MAX}$ shown in the left column of Fig. 8 by products of two lognormal spectra according to Eq. 4.

$$\frac{F_{\bar{\nu}}(\bar{\nu}_{ex},\bar{\nu}_{em})}{F_{\bar{\nu}}^{MAX}} = \exp\left\{-\frac{\ln^2\left[1+2b_{ex}\left(\bar{\nu}-\bar{\nu}_{ex}^{MAX}\right)/W_{ex}\right]}{b_{ex}^2/\ln 2}\right\}\exp\left\{-\frac{\ln^2\left[1+2b_{em}\left(\bar{\nu}-\bar{\nu}_{em}^{MAX}\right)/W_{em}\right]}{b_{em}^2/\ln 2}\right\}$$

(4)

Considering $F_{\bar{\nu}}(\bar{\nu}_{ex},\bar{\nu}_{em}) = \varepsilon(\bar{\nu}_{ex})\Phi_{em} f_{\bar{\nu}}(\bar{\nu}_{em})$ with the cross section of absorption $\varepsilon(\bar{\nu}_{ex})$ and the quantum yield Φ_{em} and normalized quantum spectrum of emission $f_{\bar{\nu}}(\bar{\nu}_{em})$, the product function of Eq. 4 accounts for the spectral shape of absorption and emission. The five sets of the six spectral parameters are summarized in Table 1, the fitted 2D spectra are displayed in the left column of Fig.10 We note a distinct asymmetry of the 2D spectra, in particular for ANNINE-5 and ANNINE-6 with steep slopes towards the red in excitation and towards the blue in emission. To illustrate the quality of the fit, we check onedimensional sections along the axes of excitation and emission. The upper graphs of Fig.11 show the data and the fit function. The good agreement - except for high wavenumbers of excitation where the contribution of the S_0/S_2 transition is significant – confirms the validity of the approach. Also the onedimensional spectra exhibit the steep slopes in the red of the excitation band and in the blue of the emission band.

Table 1

Voltage sensitivity. The spectrum of voltage sensitivity $S_V(\bar{\nu}_{ex},\bar{\nu}_{em})$ is defined as the relative change of fluorescence intensity per change of membrane voltage according to Eq. 5.

$$S_V(\bar{\nu}_{ex},\bar{\nu}_{em}) = \frac{\Delta F_{\bar{\nu}}(\bar{\nu}_{ex},\bar{\nu}_{em})}{F_{\bar{\nu}}(\bar{\nu}_{ex},\bar{\nu}_{em})} \frac{1}{\Delta V_M} \qquad (5)$$

We obtain it by subtracting the relative spectrum $F_{\bar{\nu}}^{hyp}/F_{\bar{\nu}}^{hyp,MAX}$ at a hyperpolarized voltage from the scaled spectrum $F_{\bar{\nu}}^{dep}/F_{\bar{\nu}}^{hyp,MAX}$ at a depolarized voltage and division by $F_{\bar{\nu}}^{hyp}/F_{\bar{\nu}}^{hyp,MAX}$ and the voltage difference ΔV_M. The results - scaled to a voltage $\Delta V_M = 100mV$ - are shown in the right column of Fig. 8. All sensitivity spectra exhibit two regions: at high wavenumbers of excitation and emission, the fluorescence is enhanced, at low wavenumbers the fluorescence is reduced. Tha magnitude of this effect increaes in the homologous series RH-421, di4-ANEPBS, BNBIQ and ANNINE-5, and also in ANNINE-6. Within the limited spectral window of the measurements, the sensitivity is in the range of $\pm 10\%/100mV$ for RH-421, $\pm 15\%/100mV$ for di-4-ANEPPS, $\pm 20\%/100mV$ for BNBIQ and $\pm 25\%/100mV$ for ANNINE-5 and ANNINE-6.

Parametrized voltage sensitivity. A parametrization of voltage sensitivity is achieved by fitting the scaled spectra $F_{\bar{\nu}}^{dep}/F_{\bar{\nu}}^{hyp,MAX}$ and $F_{\bar{\nu}}^{hyp}/F_{\bar{\nu}}^{hyp,MAX}$ at the two voltages by products of lognormal functions according to Eq. 4. The resulting differences of the spectral parameters $\Delta\bar{\nu}_{ex}^{MAX}$, $\Delta\bar{\nu}_{em}^{MAX}$, ΔW_{ex}, ΔW_{em}, Δb_{ex}, Δb_{em} and ΔF_{ν}^{MAX} are small for all dyes. For that reason we can assume that the changes of the spectra are linear with respect to changes of the spectral parameters, and we are allowed to scale the parameter changes to a standard voltage change of $\Delta V_M = 100mV$ as it is typical for neuronal excitation. The resulting differences are shown in Table 2.

Table 2

Using the fit parameters from Tables 1 and 2, we reconstruct the sensitivity spectra $S_V(\bar{\nu}_{ex},\bar{\nu}_{em})$ according to Eq. 5. The results are displayed in the central column of Fig.10 in a range where the relative change of intensity is above 10%. For ANNINE-6, ANNINE-5 and BNBIQ, the fitted sensitivity spectra exhibit a distinct enhancement and reduction of fluorescence at high and low wavenumbers, respectively. In particular, we note the steep increase of negative sensitivity with decreasing wavenumber of excitation in the red corner of the 2D spectrum and the steep increase of positive sensitivity with increasing wavenumber of emission in the blue corner of the 2D spectrum. For the two styryl dyes the sensitivity spectra are more involved.

To illustrate the quality of the sensitivity spectra $S_V(\bar{\nu}_{ex},\bar{\nu}_{em})$ reconstructed from the fit of the twodimensional spectra at two voltages, we select onedimensional spectra $S_V(\bar{\nu}_{ex})$ and $S_V(\bar{\nu}_{em})$ across the sensitivity data (Fig. 3) and across the fitted spectra (Fig. 5). They are shown in Fig.11 and exhibit a good agreement, except for high excitation wavenumbers where the S_0/S_2 transition contributes and at low emission wavenumbers where the intensity is modest.

Voltage sensitivity. An electric field across a cell membrane may in principle affect the electronic structure of a bound chromophore, its vibroelectronic coupling and its interaction with the matrix. It may change the electronic 00 transition energy, the Franck-Condon factors of excitation and emission, the transition dipole moments and radiationless deactivation channels. As a result, the twodimensional fluorescence spectrum $F_{\bar{\nu}}(\bar{\nu}_{ex},\bar{\nu}_{em})=\varepsilon(\bar{\nu}_{ex})\Phi_{em}f_{\bar{\nu}}(\bar{\nu}_{em})$ may be modulated through the absorption

spectrum $\varepsilon(\bar{\nu}_{ex})$, the quantum yield of emission Φ_{em} and the normalized quantum spectrum of emission $f_{\bar{\nu}}(\bar{\nu}_{em})$. The sensitivity spectrum defined by Eq. 5 reflects changes of all these molecular parameters according to Eq. 6.

$$S_V(\bar{\nu}_{ex},\bar{\nu}_{em})=\frac{1}{\varepsilon(\bar{\nu}_{ex})}\frac{\Delta\varepsilon(\bar{\nu}_{ex})}{\Delta V_M}+\frac{1}{\Phi_{em}}\frac{\Delta\Phi_{em}}{\Delta V_M}+\frac{1}{f_{\bar{\nu}}(\bar{\nu}_{em})}\frac{\Delta f_{\bar{\nu}}(\bar{\nu}_{em})}{\Delta V_M} \qquad (6)$$

In fact, when we fit the twodimensional fluorescence spectra at two voltages by products of lognormal functions, we find that the joined amplitude $F_{\bar{\nu}}^{MAX}$ and all spectral parameters of excitation $\bar{\nu}_{ex}^{MAX}$, W_{ex}, b_{ex} and of emission $\bar{\nu}_{em}^{MAX}$, W_{em}, b_{em} are modified by an electric field as summarized in Table 2. An assigment of these parameter changes to molecular mechanisms, however, is difficult. E.g. spectral shifts $\Delta\bar{\nu}_{ex}^{MAX}$ and $\Delta\bar{\nu}_{em}^{MAX}$ may arise not only from a change of the electronic 00 energy, and amplitude changes $\Delta F_{\bar{\nu}}^{MAX}$ not only from a changed fluorescence quantum yield, but in both cases changes of spectral shape contribute, too. It is a further problem that the parameter changes $\Delta\bar{\nu}_{ex}^{MAX}$, $\Delta\bar{\nu}_{em}^{MAX}$, ΔW_{ex}, ΔW_{em}, Δb_{ex}, Δb_{em} and $\Delta F_{\bar{\nu}}^{MAX}$ are derived from a small difference of two spectra, a procedure that implies a large error. For both reasons we do not attempt to provide a detailed mechanistic interpretation of voltage-sensitivity. We consider only one aspect, the possible contribution of a molecular Stark effect.

Electrochromism of excitation. A typical feature of voltage sensitivity of all hemicyanines considered is a blue shift $\Delta\bar{\nu}_{ex}^{MAX}$ of all excitation spectra induced by a positive change ΔV_M of the membrane voltage (Table 2). That blue shift increases in the homologous series RH-421, di-4-ANEPBS, BNBIQ, ANNINE-5 and also in

ANNINE-6. To confirm the significance of that observation, we repeat the evaluation of the spectral data in terms of a product of lognormal functions (Eq. 4) with five parameters at constant spectral asymmetries b_{ex} and b_{em} and also with three parameters at constant asymmetries and constant spectral widths W_{ex} and W_{em}. The resulting spectral shifts are summarized in Table 3. Apparently, the systematic blue shift of excitation is rather insensitive to the fit procedure.

We assign the blue shift of excitation to a molecular Stark effect of the membrane bound chromophores [28-31]. Due to their amphiphilic structure, the hemicyanines may be expected to be bound to the surface of the neuron membrane with a distinct orientation [18, 19]. In that case, an intramolecular charge displacement $\Delta\mu_{EG}$ by electronic excitation from the pyridinium to the aniline moiety is directed against a change $\Delta E = \Delta V_M / d_M$ of the average electrical field in a membrane of thickness d_M as induced by a positive change ΔV_M of the membrane voltage. The expected blue shift is expressed by Eq. 7 with a projection $\cos\vartheta$ of charge displacement on the membrane normal (Planck's constant h, velocity of light c).

$$hc\,\Delta\bar{\nu}_{ex}^{MAX} = \Delta\mu_{EG}\,\Delta E\cos\vartheta \qquad (7)$$

From the experimentals shifts $\Delta\bar{\nu}_{ex}^{MAX}$ we estimate the charge displacement $\Delta\mu_{EG}\cos\vartheta$ along the membrane normal for $\Delta V_M = 100mV$ and $d_M = 4nm$. Considering the fit with seven parameters (Table 2), we obtain for RH-421, di-4-ANEPBS, BNBIQ, ANNINE-5 and ANNINE-6 values of 12, 21, 24, 31 and 39 Debye. The effective displacements of an elementary charge e_0 along the membrane normal

$(\Delta\mu_{EG}/e_0)\cos\vartheta$ are 0.24 *nm*, 0.43 *nm*, 0.51 *nm*, 0.65 *nm* and 0.81 *nm*. With respect to charge displacement, ANNINE-6 is better by factor of three than the classical styryl dye RH-421. The enhancement may be due either to a stronger intramolecular charge shift $\Delta\mu_{EG}$ or to a better orientation $\cos\vartheta$ in the membrane. A discrimination of the two effects is not possible on the basis of the present data. It may be achieved by systematic measurements of the chromophore orientation in the neuron membrane and by quantumchemical computations of the electronic structure of the chromophores.

Electrochromism and membrane solvatochromism. The assignment of a Stark effect to the electrochromic blue shift is confirmed by a consideration of solvatochromism in the neuron membrane. Due to their orientation, the chromophores at the membrane/water interface are in an extremely inhomogeneous environment that may give rise to specific solvatochromic effects with amphiphilic hemicyanines [32]. We have to distinguish the effect of local polarity and the effect of the local polarity gradient [33]. In homogeneous solvents, a changing polarity gives rise to a symmetric opposite shift of excitation and emission spectra with an invariant average wavenumber $\bar{\nu}_{00} = \left(\bar{\nu}_{ex}^{MAX} + \bar{\nu}_{em}^{MAX}\right)/2$ of the 00 energy [12]. As a consequence, a shift $\Delta\bar{\nu}_{00} = \bar{\nu}_{00}^{mem} - \bar{\nu}_{00}$ of the average wavenumber in the membrane may be considered as a quantitative indicator for an effect of the polarity gradient. The wavenumbers $\bar{\nu}_{00}^{mem}$ in the neuron membrane and the 00 energies $\bar{\nu}_{00}$ in bulk solvents [12, 23] are summarized in Table 4. There is indeed a large blue shift for all dyes that increases in the series RH-421, di-4-ANEPBS, BNBIQ, ANNINE-5 and ANNINE-6.

We may expect that the solvatochromic effect of the polarity gradient is related to the intramolecular charge displacement $\Delta\mu_{EG}\cos\vartheta$ across the polarity gradient. Thus we express the blue shift $\Delta\bar{\nu}_{00}$ by Eq. 8

$$hc\Delta\bar{\nu}_{00} = E_0\,\Delta\mu_{EG}\cos\vartheta \qquad (8)$$

The effective internal electric field E_0 characterizes the strength of the gradient. On the basis of Eq. 8 the increasing solvatochromic blue shifts $\Delta\bar{\nu}_{00}$ in the series RH-421, di-4-ANEPBS, BNBIQ, ANNINE-5 and ANNINE-6 reflect an increasing charge displacement $\Delta\mu_{EG}\cos\vartheta$. As electrochromism caused by a Stark effect and solvatochromism induced by a polarity gradient are both proportional to $\Delta\mu_{EG}\cos\vartheta$, we expect a proportionality of the electrochromic shift $\Delta\bar{\nu}_{ex}^{MAX}$ and the solvatochromic shift $\Delta\bar{\nu}_{00}$. In fact, Fig. 12 shows such a linear correlation with $\Delta\bar{\nu}_{ex}^{MAX} = 0.045\Delta\bar{\nu}_{00}$ and confirms the consistency of our interpretations.

Ideal Stark effect probes. A molecular Stark effect may affect not only the excitation but also the emission of a dye. The resulting spectral shift is described by Eq. 9.

$$hc\Delta\bar{\nu}_{em}^{MAX} = \Delta\mu_{EG}\,\Delta E\cos\vartheta \qquad (9)$$

In fact, for BNBIQ, ANNINE-5 and ANNINE-6 we observe electrochromic blue shifts of emission that are almost identical to those of excitation (Table 3). We assign that correspondence to an identical molecular Stark effect for excitation and emission

with an identical charge shift $\Delta\mu_{EG}\cos\vartheta$ due to an identical electronic transition and an similar orientation of the chromophore for excitation and emission.

To test, how far the Stark effect of excitation and emission dominates the voltage sensitivity of BNBIQ, ANNINE-5 and ANNINE-6, we compute the sensitivity spectrum $S_V(\bar{\nu}_{ex},\bar{\nu}_{em})$ for an identical blue shift of excitation and emission at invariant spectral shape and amplitude with $\Delta W_{ex}=\Delta W_{em}=\Delta b_{ex}=\Delta b_{em}=\Delta F_{\bar{\nu}}^{MAX}=0$ using Eqs. 4 and 5. Choosing the averages $\Delta\bar{\nu}_{ex,em}^{MAX}=\left(\Delta\bar{\nu}_{ex}^{MAX}+\Delta\bar{\nu}_{em}^{MAX}\right)/2$ of the blue shifts from Table 2, we obtain Fig.13 The computed voltage sensitivities are most similar to the fitted spectra in the central column of Fig10; BNBIQ, ANNINE-5 and ANNINE-6 are almost ideal Stark probes for voltage changes in nerve cells.

When we express the voltage sensitivity for a pure Stark effect by Eq. 6, considering a small spectral shift $\Delta\bar{\nu}_{ex,em}$, we obtain Eq. 10 in terms of the derivatives of the absorption and emission spectrum $\varepsilon'=d\varepsilon/d\bar{\nu}_{ex}$ and $f'=df/d\bar{\nu}_{em}$.

$$S_V(\bar{\nu}_{ex},\bar{\nu}_{em})=\frac{\Delta\bar{\nu}_{ex,em}}{\Delta V_M}\left[\frac{\varepsilon'(\bar{\nu}_{ex})}{\varepsilon(\bar{\nu}_{ex})}+\frac{f_{\bar{\nu}}'(\bar{\nu}_{em})}{f_{\bar{\nu}}(\bar{\nu}_{em})}\right] \qquad (10)$$

The voltage sensitivity $S_V(\bar{\nu}_{ex},\bar{\nu}_{em})$ depends not only on the spectral shift caused by the intramolecular charge displacement, but also on the shapes of the absorption and emission spectra that are determined by the Franck-Condon factors of the vibroelectronic transitions. The relative slope of the excitation spectrum for ANNINE-5 and ANNINE-6 is highest and positive in the red, whereas the relative slope of the

emission spectrum is highest and negative in the blue as shown in Figs.10 and 11 The relative slopes are distinctly smaller in the blue of excitation and in the red of emission. However, due to their different sign, the optimal sensitivitites with respect to excitation and emission cannot be combined. For optical recording we may choose the red corner of the twodimensional sensitivity spectra as illustrated in Fig.10 In accordance with Eq. 10, the sensitivity increases dramatically in the red of excitation but only modestly in the red of emission as illustrated also by the onedimensional spectra of Fig.11.

Styryl dyes. For the styryl dyes di-4-ANEPBS and RH421 the spectral shifts of excitation and emission are not identical (Table 2). The blue shift of emission for di-4-ANEPBS is about 50% of the blue shift of excitation, and RH-421 even exhibits a red shift of emission. These results do not depend on the fit procedure (Table 3). Apparently, with these dyes the emission is affected by other effects besides a Stark effect. Possibly, the electrical field changes position and orientation of the excited chromophores, resulting in a field induced solvatochromic red shift of emission that is superposed to a Stark effect.

Optical recording. The sensitivity function $S_V(\bar{\nu}_{ex},\bar{\nu}_{em})$ reflects molecular features of the membrane bound dye according to Eq. 6. However, the photodiode signal $\Delta P(\bar{\nu}_{ex},\bar{\nu}_{em})$ due to a voltage change ΔV_M of neuronal activity in an experimental setup of optical recording does not only depend on voltage sensitivity, but also on staining, illumination and detection. Considering Eqs. 1 and 2 we obtain Eq. 11: a high response requires a large observed membrane area A_{mem}, a high density of dye molecules per unit area n_{dye}, a high quantum intensity of illumination $I_{\bar{\nu}}^{ill}(\bar{\nu}_{ex})\Delta\bar{\nu}_{ex}$, a high efficiency of the detection system $T^{rec}(\bar{\nu}_{em})\Delta\bar{\nu}_{em}$, a high voltage sensitivity

$S_V(\bar{\nu}_{ex},\bar{\nu}_{em})$ and - considering $F_{\bar{\nu}}(\bar{\nu}_{ex},\bar{\nu}_{em})=\varepsilon(\bar{\nu}_{ex})f_{\bar{\nu}}(\bar{\nu}_{em})\Phi_{em}$ - a high cross section of absorption $\varepsilon(\bar{\nu}_{ex})$ and a high yield of fluorescence $f_{\bar{\nu}}(\bar{\nu}_{em})\Phi_{em}$.

$$\Delta P(\bar{\nu}_{ex},\bar{\nu}_{em})=\Delta V_M A_{mem} n_{dye}\cdot I^{ill}_{\bar{\nu}}(\bar{\nu}_{ex})\Delta\bar{\nu}_{ex}\cdot S_V(\bar{\nu}_{ex},\bar{\nu}_{em})\cdot F_{\bar{\nu}}(\bar{\nu}_{ex},\bar{\nu}_{em})\cdot T^{rec}(\bar{\nu}_{em})\Delta\bar{\nu}_{em} \quad (11)$$

We consider an illumination with a narrow spectral band width at a wavenumber $\bar{\nu}^*_{ex}$ with an integral intensity $I^{ill}=\int I^{ill}_{\bar{\nu}}(\bar{\nu}_{ex})d\bar{\nu}_{ex}$ and a detection with constant efficiency $T^{rec}(\bar{\nu}_{em})=T^{rec}$ within the spectral limits $\bar{\nu}^A_{em}$ and $\bar{\nu}^B_{em}$ of recording. The total photodiode signal is given by Eq. 12.

$$\Delta P=\Delta V_M A_{mem} n_{dye} I^{ill}\, T^{rec}\int_{\bar{\nu}emA}^{\bar{\nu}emB} F_{\bar{\nu}}(\bar{\nu}^*_{ex},\bar{\nu}_{em})S_V(\bar{\nu}^*_{ex},\bar{\nu}_{em})\,d\bar{\nu}_{em} \quad (12)$$

An optimal signal is achieved by good staining, high illumination intensity, high detector sensitivity and proper selection of the excitation wavenumber $\bar{\nu}^*_{ex}$ and the emission filters $\bar{\nu}^A_{em}$ and $\bar{\nu}^B_{em}$ to attain a large integral over the product of sensitivity spectrum and fluorescence spectrum. For illustration the normalized response spectrum $R_V(\bar{\nu}_{ex},\bar{\nu}_{em})=S_V(\bar{\nu}_{ex},\bar{\nu}_{em})F_{\bar{\nu}}(\bar{\nu}_{ex},\bar{\nu}_{em})/F^{MAX}_{\bar{\nu}}$ is plotted in the right column of Fig. 10. Highest negative integrals are found in the red corner of the spectrum with an excitation wavenumber $\bar{\nu}^*_{ex}$ at the minimum of $R_V(\bar{\nu}_{ex},\bar{\nu}_{em})$ and with emission filters $\bar{\nu}^A_{em}$ and $\bar{\nu}^B_{em}$ excluding the region of positive response. The highest reponse increases significantly in the series RH-421, di-4-ANEPBS, BNBIQ, ANNINE-5 and ANNINE-6.

Signal-to-noise. The total response expressed by Eq. 12 reflects the signal-to-noise ratio only if the noise is constant, e.g. dominated by the electronic amplifier. If the shot noise of photons dominates [34], we have to consider a noise level $N=\sqrt{P/2\tau_D}$

that depends on the total photon counts P and the time constant of the detector τ_D.

With $P = A_{mem} n_{dye} I^{ill} T^{rec} \int_{\bar{\nu}emA}^{\bar{\nu}emB} F_{\bar{\nu}}(\bar{\nu}_{ex}^{*}, \bar{\nu}_{em}) d\bar{\nu}_{em}$ we obtain Eq. 13.

$$\frac{\Delta P}{N} = \Delta V_M \sqrt{2\tau_D A_{mem} I^{ill} n_{dye} T^{rec} \Phi_{em}} \frac{\int_{\bar{\nu}emA}^{\bar{\nu}emB} F_{\bar{\nu}}(\bar{\nu}_{ex}^{*}, \bar{\nu}_{em}) S_{\bar{\nu}}(\bar{\nu}_{ex}^{*}, \bar{\nu}_{em}) d\bar{\nu}_{em}}{\sqrt{\int_{\bar{\nu}emA}^{\bar{\nu}emB} F_{\bar{\nu}}(\bar{\nu}_{ex}^{*}, \bar{\nu}_{em}) d\bar{\nu}_{em}}} \qquad (13)$$

In optimizing the signal-to-noise ratio, we have to take into account the role of photobleaching and phototoxicity of the dyes. These effects impair optical recording because dyes and cells fade away by illumination. Both photochemical processes are determined by the number of excitations per unit time. The signal-to-noise ratio must be optimized with the constraint of a certain number of excitations per unit time that is tolerable for a certain experiment. When we express the fluorescence spectrum by $F_{\bar{\nu}}(\bar{\nu}_{ex}^{*}, \bar{\nu}_{em}) = \varepsilon(\bar{\nu}_{ex}^{*}) \Phi_{em} f_{\bar{\nu}}(\bar{\nu}_{em})$ we obtain Eq 14.

$$\frac{\Delta P}{N} = \Delta V_M \sqrt{2\tau_D A_{mem}} \sqrt{I^{ill} n_{dye} \varepsilon(\bar{\nu}_{ex}^{*})} \sqrt{T^{rec} \Phi_{em}} \frac{\int_{\bar{\nu}emA}^{\bar{\nu}emB} f_{\bar{\nu}}(\bar{\nu}_{em}) S_{\bar{\nu}}(\bar{\nu}_{ex}^{*}, \bar{\nu}_{em}) d\bar{\nu}_{em}}{\sqrt{\int_{\bar{\nu}emA}^{\bar{\nu}emB} f_{\bar{\nu}}(\bar{\nu}_{em}) d\bar{\nu}_{em}}} \qquad (14)$$

Here the signal-to-noise ratio is expressed in terms of (i) the spatiotemporal resolution $\tau_D A_{mem}$ of the setup, (ii) the number of excitations per area and time $I^{ill} n_{dye} \varepsilon(\bar{\nu}_{ex}^{*})$, (iii) the yield of detected quanta $T^{rec} \Phi_{em}$ and (iv) the sensitivity function $S_{\bar{\nu}}(\bar{\nu}_{ex}^{*}, \bar{\nu}_{em})$ weighted by the fluorescence spectrum $f_{\bar{\nu}}(\bar{\nu}_{em})$ within the spectral limits of detection. With a constraint $I^{ill} \varepsilon(\bar{\nu}_{ex}^{*}) = const.$ the choice of an optimal wavenumber of excitation $\bar{\nu}_{ex}^{*}$ and of optimal emission filters $\bar{\nu}_{em}^{A}$ and $\bar{\nu}_{em}^{B}$ is determined by a weighted sensitivity function $\langle S_V(\bar{\nu}_{ex}^{*}) \rangle$ defined by Eq. 15.

$$\left\langle S_V\left(\bar{\nu}_{ex}^{\bullet}\right)\right\rangle = \frac{\int_{\bar{\nu}emA}^{\bar{\nu}emB} f_{\bar{\nu}}\left(\bar{\nu}_{em}\right) S_{\bar{\nu}}\left(\bar{\nu}_{ex}^{\bullet}, \bar{\nu}_{em}\right) d\bar{\nu}_{em}}{\sqrt{\int_{\bar{\nu}emA}^{\bar{\nu}emB} f_{\bar{\nu}}\left(\bar{\nu}_{em}\right) d\bar{\nu}_{em}}} \qquad (15)$$

For the ANNINE dyes, the sensitivity $S_{\bar{\nu}}\left(\bar{\nu}_{ex}^{\bullet}, \bar{\nu}_{em}\right)$ (Fig. 5) reaches largest negative values in the red corner of the spectrum. We expect a high signal-to-noise ratio when we excite monochromatically at a rather low wavenumber $\bar{\nu}_{ex}^{\bullet}$. To keep $I^{III}\varepsilon\left(\bar{\nu}_{ex}^{\bullet}\right)$ constant, we have to compensate the low cross section of absorption by an enhanced illumination intensity. Of course, we have to limit the detection to the range of negative response. For illustration, the weighted sensitivity function $\left\langle S_V\left(\bar{\nu}_{ex}^{\bullet}\right)\right\rangle$ obtained from the data is plotted in Fig.14 for ANNINE-6 versus the wavenumber of illumination.

These features of the signal-to-noise ratio for $I^{III}\varepsilon\left(\bar{\nu}_{ex}^{\bullet}\right) = const.$ are expected for a Stark effect. When we insert Eq. 10 in Eq. 15 we obtain Eq. 16.

$$\left\langle S_V\left(\bar{\nu}_{ex}^{\bullet}\right)\right\rangle = \frac{\Delta\bar{\nu}_{ex,em}}{\Delta\bar{\nu}_M}\sqrt{\int_{\bar{\nu}emA}^{\bar{\nu}emB} f_{\bar{\nu}}\left(\bar{\nu}_{em}\right) d\bar{\nu}_{em}}\left\{\frac{\varepsilon'\left(\bar{\nu}_{ex}^{\bullet}\right)}{\varepsilon\left(\bar{\nu}_{ex}^{\bullet}\right)} + \frac{\int_{\bar{\nu}emA}^{\bar{\nu}emB} f_{\bar{\nu}}'\left(\bar{\nu}_{em}\right) d\bar{\nu}_{em}}{\int_{\bar{\nu}emA}^{\bar{\nu}emB} f_{\bar{\nu}}\left(\bar{\nu}_{em}\right) d\bar{\nu}_{em}}\right\} \qquad (16)$$

When we choose an excitation wavenumber in the red where the relative slope of the excitation spectrum is steep, we expect an increasing contribution of the Stark effect of excitation at a rather invariant contribution of the Stark effect of emission. Thus we expect an increasing signal-to-noise ratio for an illumination $\bar{\nu}_{ex}^{\bullet}$ at the red end of the excitation spectrum. Of course, the signal-to-noise ratio is proportional to the spectral shift by the Stark effect.

The anellated hemicyanine dyes ANNINE-5 and ANNINE-6 exhibit voltage sensitivities in a neuron membrane that are distinctly higher than those of the classical styryl dyes. These novel probes rely on a well defined physical mechanism, the molecular Stark effect. Their excellence for optical recording of neuronal excitation is due to a large intramolecular charge shift in connection with suitable Franck-Condon factors of vibroelectronic transitions and a high quantum yield of fluorescence. Further improvements of the voltage sensitive dyes must be directed towards higher photochemical stability and lower phototoxicity and towards a selective staining of individual cells in a tissue.

References of example 3 :

(1) Bullen, A.; Saggau, P. Optical Recording from Individual Neurons in Culture. In: *Modern Techniques in Neuroscience Research*; 1 ed.; Johansson, H., Ed.; Springer-Verlag: Berlin, 1999; pp 89.

(2) Sinha, S. R.; Saggau, P. Optical Recording from Populations of Neurons in Brain Slices. In *Modern Techniques in Neuroscience Research*; 1 ed.; Johansson, H., Ed.; Springer-Verlag: Berlin, 1999; pp 459.

(3) Grinvald, A.; Shoham, D.; Shmuel, A.; Glaser, D.; Vanzetta, I.; Shtoyerman, E.; Slovin, H.; Wijnbergen, C.; Hildesheim, R.; Arieli, A. In-vivo Optical Imaging of Cortical Architecture and Dynamics. In *Modern Techniques in Neuroscience Research*; 1 ed.; Johansson, H., Ed.; Springer-Verlag: Berlin, 1999; pp 893.

(4) Tasaki, I.; Watanabe, A.; Sandlin, R.; Carnay, L. *Proc. Natl. Acad. Sci. USA* 1968, *61*, 883.

(5) Cohen, L. B.; Salzberg, B. M.; Davila, H. V.; Ross, W. N.; Landowne, D.; Waggoner, A. S.; Wang, C. H. *J. Membrane Biol.* 1974, *19*, 1.

(6) Cohen, L. B.; Salzberg, B. M. *Rev. Physiol. Biochem. Pharmacol.* 1978, *83*, 35.

(7) Loew, L. M.; Bonneville, G. W.; Surow, J. *Biochemistry* 1978, *17*, 4065.

(8) Loew, L. M.; Simpson, L. L. *Biophys. J.* 1981, *34*, 353.

(9) Fluhler, E.; Burnham, V. G.; Loew, L. M. *Biochemistry* 1985, *24*, 5749.

(10) Grinvald, A.; Hildesheim, R.; Farber, I. C.; Anglister, L. *Biophys. J.* 1982, *39*, 301.

(11) Grinvald, A.; Fine, A.; Farber, I. C.; Hildesheim, R. *Biophys. J.* **1983**, *42*, 195.

(12) Fromherz, P. *J. Phys. Chem.* **1995**, *99*, 7188.

(13) Fromherz, P.; Lambacher, A. *Biochim. Biophys. Acta* **1991**, *1068*, 149.

(14) Fromherz, P.; Muller, C. O. *Biochim. Biophys. Acta* **1993**, *1150*, 111.

(15) Ephardt, H.; Fromherz, P. *J. Phys. Chem.* **1989**, *93*, 7717.

(16) Rocker, C.; Heilemann, A.; Fromherz, P. *J. Phys. Chem.* **1996**, *100*, 12172.

(17) Fromherz, P.; Rocker, C. *Ber. Bunsen-Ges. Phys. Chem.* **1994**, *98*, 128.

(18) Visser, N. V.; van Hoek, A.; Visser, A. J.; Frank, J.; Apell, H. J.; Clarke, R. J. *Biochemistry* **1995**, *34*, 11777.

(19) Lambacher, A.; Fromherz, P. *J. Phys. Chem. B* **2001**, *105*, 343.

(20) Gupta, R. K.; Salzberg, B. M.; Grinvald, A.; Cohen, L. B.; Kamino, K.; Lesher, S.; Boyle, M. B.; Waggoner, A. S.; Wang, C. H. *J. Membrane Biol.* **1981**, *58*, 123.

(21) Fromherz, P.; Dambacher, K. H.; Ephardt, H.; Lambacher, A.; Muller, C. O.; Neigl, R.; Schaden, H.; Schenk, O.; Vetter, T. *Ber. Bunsen-Ges. Phys. Chem.* **1991**, *95*, 1333.

(22) Ephardt, H.; Fromherz, P. *J. Phys. Chem.* **1993**, *97*, 4540.

(23) Huebener, G.; Lambacher, A.; Fromherz, P. *J. Phys. Chem. B submitted* **2003**.

(24) Dietzel, I. D.; Drapeau, P.; Nicholls, J. G. *J. Physiol. (Lond.)* **1986**, *372*, 191.

(25) Meyer, E.; Muller, C. O.; Fromherz, P. *Eur. J. Neurosci.* **1997**, *9*, 778.

(26) Hamill, O. P.; Marty, A.; Neher, E.; Sakmann, B.; Sigworth, F. J. *Pflugers Arch. Physiol.* **1981**, *391*, 85.

(27) Siano, D. B.; Metzler, D. E. *J. Chem. Phys.* **1969**, *51*, 1856.

(28) Junge, W.; Witt, H. T. *Z. Naturforsch. B* **1968**, *B 23*, 244.

(29) Bucher, H.; Wiegand, J.; Snavely, B. B.; Beck, K. H.; Kuhn, H. *Chem. Phys. Lett.* **1969**, *3*, 508.

(30) Reich, R.; Schmidt, S. *Ber. Bunsen-Ges. Phys. Chem.* **1972**, *76*, 589.

(31) Schmidt, S.; Reich, R. *Ber. Bunsen-Ges. Phys. Chem.* **1972**, *76*, 1202.

(32) Loew, L. M.; Simpson, L.; Hassner, A.; Alexanian, V. *J. Am. Chem. Soc.* **1979**, *101*, 5439.

(33) Ephardt, H.; Fromherz, P. *J. Phys. Chem.* **1991**, *95*, 6792.

(34) Knopfel, T.; Fromherz, P. *Z. Naturforsch. C* **1987**, *42*, 986.

Example 4:

LARGE VOLTAGE-SENSITIVE DYE SIGNALS MEASURED WITH ONE AND TWO-PHOTON EXCITATION

ANNINE-6 is a new, completely anellated hemicyanine dye. Two-dimensional sensitivity spectra suggest the use of the extreme red edge of the excitation spectrum to achieve large relative fluorescence changes in response to membrane voltage changes. Several biological preparations were used for testing. First, HEK293 cells were stained by bath application of the dye. Alternating external electric fields generated by applying voltages between two Ag/AgCl-wires in a closed chamber (1). To achieve the high light intensities, which are necessary to excite the dye at the very red edge of the excitation spectrum, we used laser scanning microscopes with Ar-Ion Laser for one-photon excitation (488nm, 514nm) and Ti:Sapphire Laser for two-photon excitation (976nm). The fluorescence changes measured with 1kHz line scans followed the applied voltage, which was alternated every 10 ms, without discernible delay. We found relative fluorescence increases of more that 60%/100mV for hyperpolarizing membrane potential changes and decreases of more than 40%/100mV for depolarizing membrane potential changes at 514nm excitation wavelength. The asymmetry of the fluorescence change is expected given the spectral shape and a pure electrochromic spectral shift. We found changes of +40%/100mV and -30%/100mV both for one-photon excitation at 488nm and two-photon excitation at 976nm . Preliminary measurements from cultured hippocampal slices using a soluble variant of ANNINE-6 show fast fluorescence changes of up to 8% upon stimulation of the Schaffer collaterals in CA1.

(1) D. Gross, L.M. Loew and W. Webb. Biophys.J., 50: 339-348, 1986.

Claims

1. A method of determining voltage changes by means of a voltage-sensitive dye, characterized in that the voltage-sensitive dye is irradiated with light having a wavelength at which the dye has an absorption ≤ 20% of its absorption maximum and the fluorescence caused by irradiation with light is measured.

2. The method according to claim 1, characterized in that the wavelength of the irradiated light is such that the dye has an absorption ≤ 2% of its absorption maximum at said wavelength.

3. The method according to claim 1,characterized in that the wavelength of the irradiated light is in the longer wavelength range, related to the absorption maximum.

4. The method according to any of the preceding claims, characterized in that an increase or decrease of fluorescence is measured.

5. The method according to any of the preceding claims,characterized in that it is used to determine voltage changes in cells.

6. The method according to any of the preceding claims, characterized in that it is used to determine voltage changes in membranes, especially cell membranes.

7. The method according to any of the preceding claims, characterized in that ANNINE-4, ANNINE-5, ANNINE-6 or ANNINE-7 is used as a voltage-sensitive dye.

8. The method according to claim 8, characterized in that a change of fluorescence radiation caused by the Stark effect is measured.

9. The method according to any of the preceding claims, characterized in that a two-photon excitation is effected.

Abstract

The present invention relates to a method of determining voltage changes, e.g. in cell membranes, by means of a voltage-sensitive dye.

mh 26.06.2003

	$\bar{\nu}_{ex}^{MAX}$ [cm^{-1}]	$\bar{\nu}_{em}^{MAX}$ [cm^{-1}]	W_{ex} [cm^{-1}]	W_{em} [cm^{-1}]	b_{ex}	b_{em}
RH-421	20249	15417	4185	3239	0.340	-0.025
di-4-ANEPBS	21199	16390	4176	3292	0.404	-0.226
BNBIQ	22298	17125	4327	3471	0.413	-0.219
ANNINE-5	23155	18419	3986	3427	0.492	-0.289
ANNINE-6	23673	17456	4326	3688	0.321	-0.206

Table 1. Spectral parameters of excitation and emission spectra for the S_0/S_1 transition of hemicyanine dyes in neuron membrane. The spectral maxima $\bar{\nu}_{ex}^{MAX}$ and $\bar{\nu}_{em}^{MAX}$, the spectral widths W_{ex} and W_{em} and the spectral asymmetries b_{ex} and b_{em} are obtained from twodimensional fluorescence spectra at a voltage of $V_M = -70mV$ by fitting products of two lognormal functions.

	$\Delta\bar{\nu}_{ex}^{MAX}$ [cm^{-1}]	$\Delta\bar{\nu}_{em}^{MAX}$ [cm^{-1}]	ΔW_{ex} [cm^{-1}]	ΔW_{em} [cm^{-1}]	Δb_{ex}	Δb_{em}	$\Delta F_{\bar{\nu}}^{MAX}$
RH-421	47	-18	-49	54	0.022	0.029	-0.039
di-4-ANEPBS	90	45	38	83	-0.024	0.006	-0.033
BNBIQ	103	99	8	24	-0.009	-0.014	-0.011
ANNINE-5	132	132	12	20	0.002	-0.016	-0.015
ANNINE-6	163	170	---	-19	---	0.022	0.018

Table 2. Voltage sensitivity of the spectral parameters of excitation and emission for the S_0/S_1 transition of the hemicyanine dyes in a neuron membrane. Twodimensional spectra of fluorescence are fitted with products of two lognormal functions at two different voltages. The changes of the spectral parameters - of the maxima $\Delta\bar{\nu}_{ex}^{MAX}$, $\Delta\bar{\nu}_{em}^{MAX}$, of the widths ΔW_{ex}, ΔW_{em}, of the asymmetries Δb_{ex} and Δb_{em}, and of the amplitude $\Delta F_{\bar{\nu}}^{MAX}$ - are scaled to a voltage change of $\Delta V_M = 100mV$. For ANNINE-6 the width and asymmetry of excitation was held constant because of an overlap with S_0/S_2 excitation.

	$\Delta\bar{V}_{ex}^{MAX}$ [cm^{-1}]			$\Delta\bar{V}_{em}^{MAX}$ [cm^{-1}]		
	7 param	5 param	3 param	7 param	5 param	3 param
RH-421	47	46	47	-18	-3	-6
di-4-ANEPBS	90	78	78	45	43	42
BNBIQ	103	97	96	99	91	91
ANNINE-5	132	132	134	132	123	123
ANNINE-6	163	163	163	170	159	159

Table 3. Spectral shifts of excitation and emission by a voltage change of $\Delta V_M = 100mV$. Twodimensional fluorescence spectra at two different voltages are fitted with products of two lognormal functions. The changes of the spectral maxima $\Delta\bar{V}_{ex}^{MAX}$ and $\Delta\bar{V}_{em}^{MAX}$ are shown for (i) a fit with seven changing spectral parameters (maxima, widths, spectral asymmetries, amplitude), (ii) a fit with five changing spectral parameters (maxima, widths, amplitude) and (iii) a fit with three changing spectral parameters (maxima, amplitude).

	$\bar{\nu}_{00}^{mem}$ [cm^{-1}]	$\bar{\nu}_{00}$ [cm^{-1}]	$\Delta\bar{\nu}_{00}$ [cm^{-1}]	$\Delta\bar{\nu}_{ex}^{MAX}$ [cm^{-1}]
RH-421	17833	16500	1333	47
di-4-ANEPBS	18795	16800	1995	90
BNBIQ	19712	17200	2512	103
ANNINE-5	20787	17900	2888	132
ANNINE-6	20565	17400	3165	163

Table 4. Membrane solvatochromism and electrochromism. The averages of the maxima of excitation and emission in the neuron membrane $\bar{\nu}_{00}^{mem} = \left(\bar{\nu}_{ex}^{MAX} - \bar{\nu}_{em}^{MAX}\right)/2$, the 00 energies $\bar{\nu}_{00}$ in bulk solvents, the solvatochromic blue shifts $\Delta\bar{\nu}_{00} = \bar{\nu}_{00}^{mem} - \bar{\nu}_{00}$ and the electrochromic blue shifts of excitation $\Delta\bar{\nu}_{ex}^{MAX}$ for an applied voltage change $\Delta V_M = 100mV$ in the neuron are shown. The $\bar{\nu}_{00}$ in bulk solvents are for RH-160 instead of 421 and for di-4-ANEPPS instead of di-4-ANEPBS.

5125

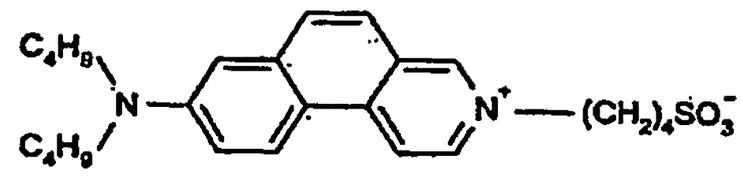

ANNINE-3

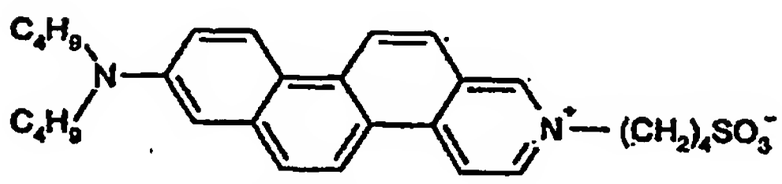

ANNINE-4

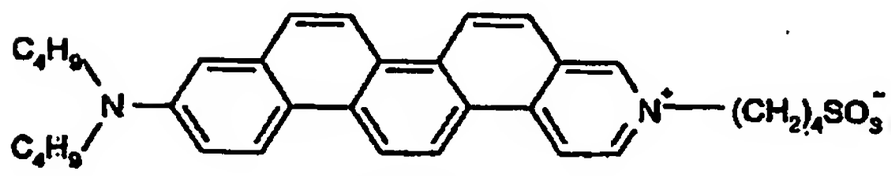

ANNINE-5

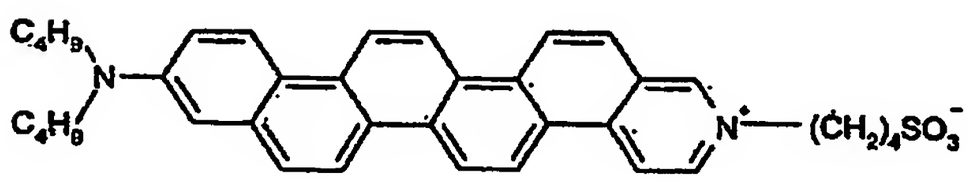

ANNINE-6

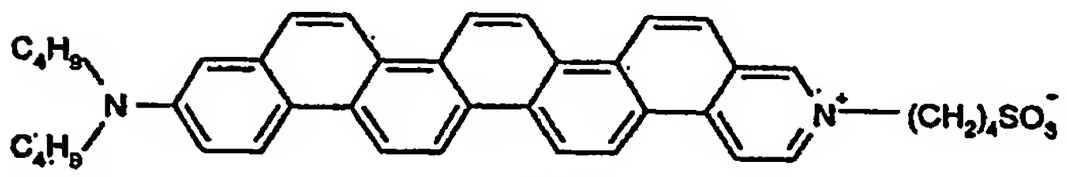

ANNINE-7

Fig. 1: Hemicyanine dyes with three to seven lineary anellated benzene rings.

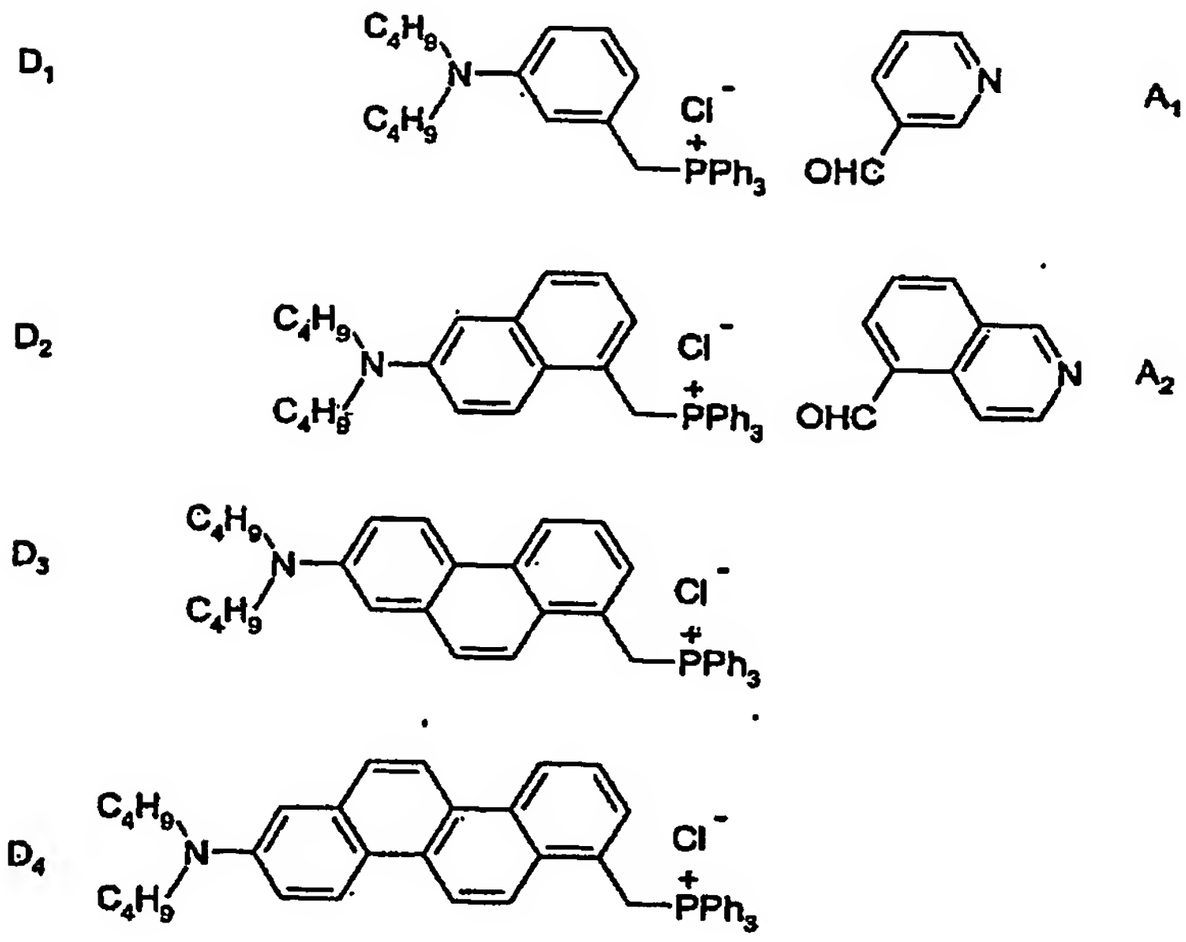

Fig. 2. Scheme of synthesis of the ANNINE dyes. The donor moieties D1 – D4 and the acceptor moieties A1 and A2 are synthetized separately. The chromphores are formed in a Wittig reaction and by subsequent ring closure in a photochemical reaction. Finally butylsulfonate groups are attached.

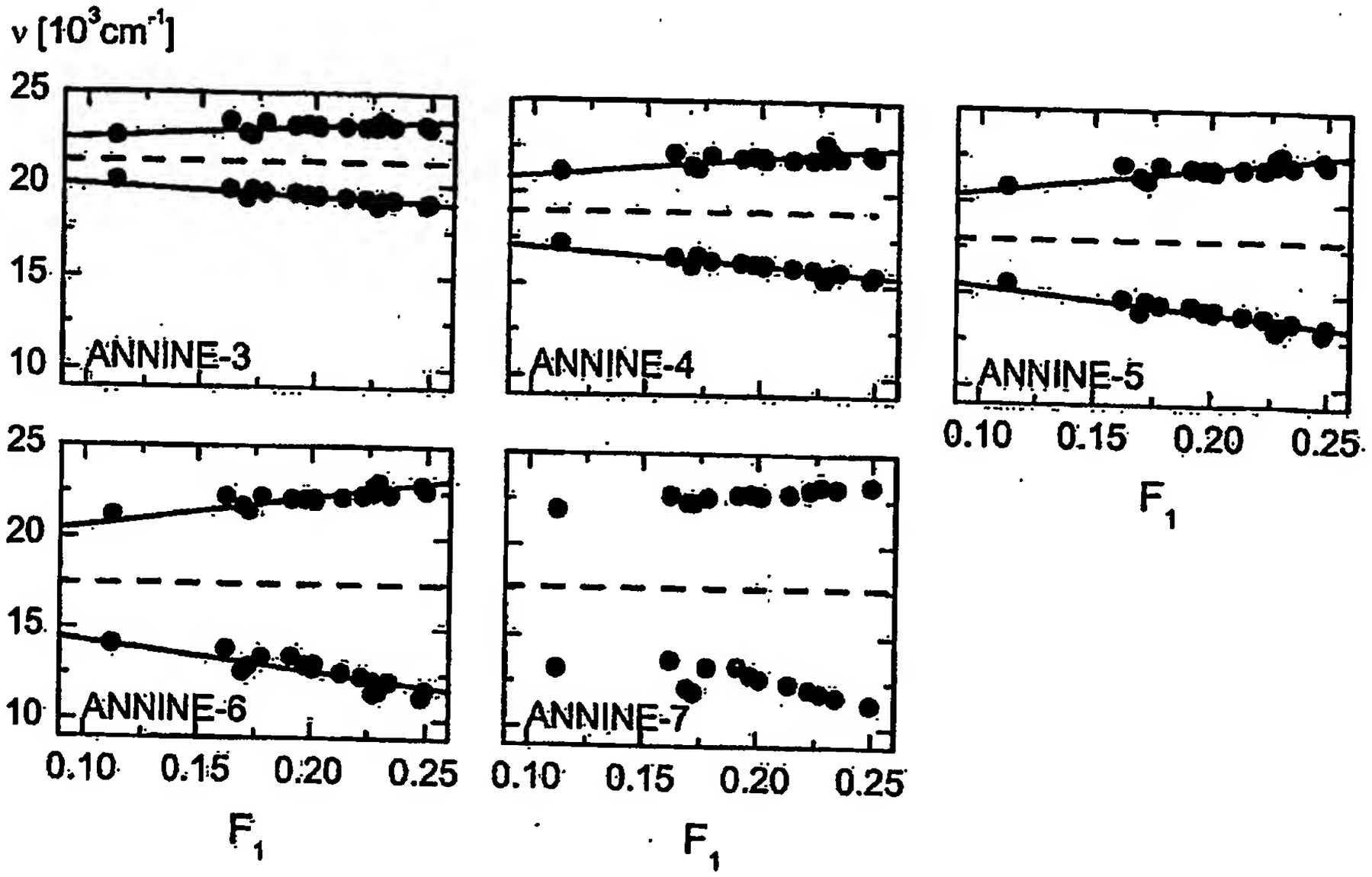

Fig. 3. Wavenumbers. Spectral data of ANNINE dyes in polar solvents. The maxima of the absorption spectra (wavenumber $\bar{\nu}_{ex}$, upper dots) and the fluorescence spectra (wavenumber $\bar{\nu}_{em}$, lower dots) are plotted versus the polarity function F_1 of 17 solvents. The straight lines are obtained from the fit of $(\bar{\nu}_{ex}+\bar{\nu}_{em})/2$ and $(\bar{\nu}_{ex}-\bar{\nu}_{em})/2$ in Fig. 4 according to a monopole-dipole model. The dashed lines are the averages of the fitted relations of excitation and emission.

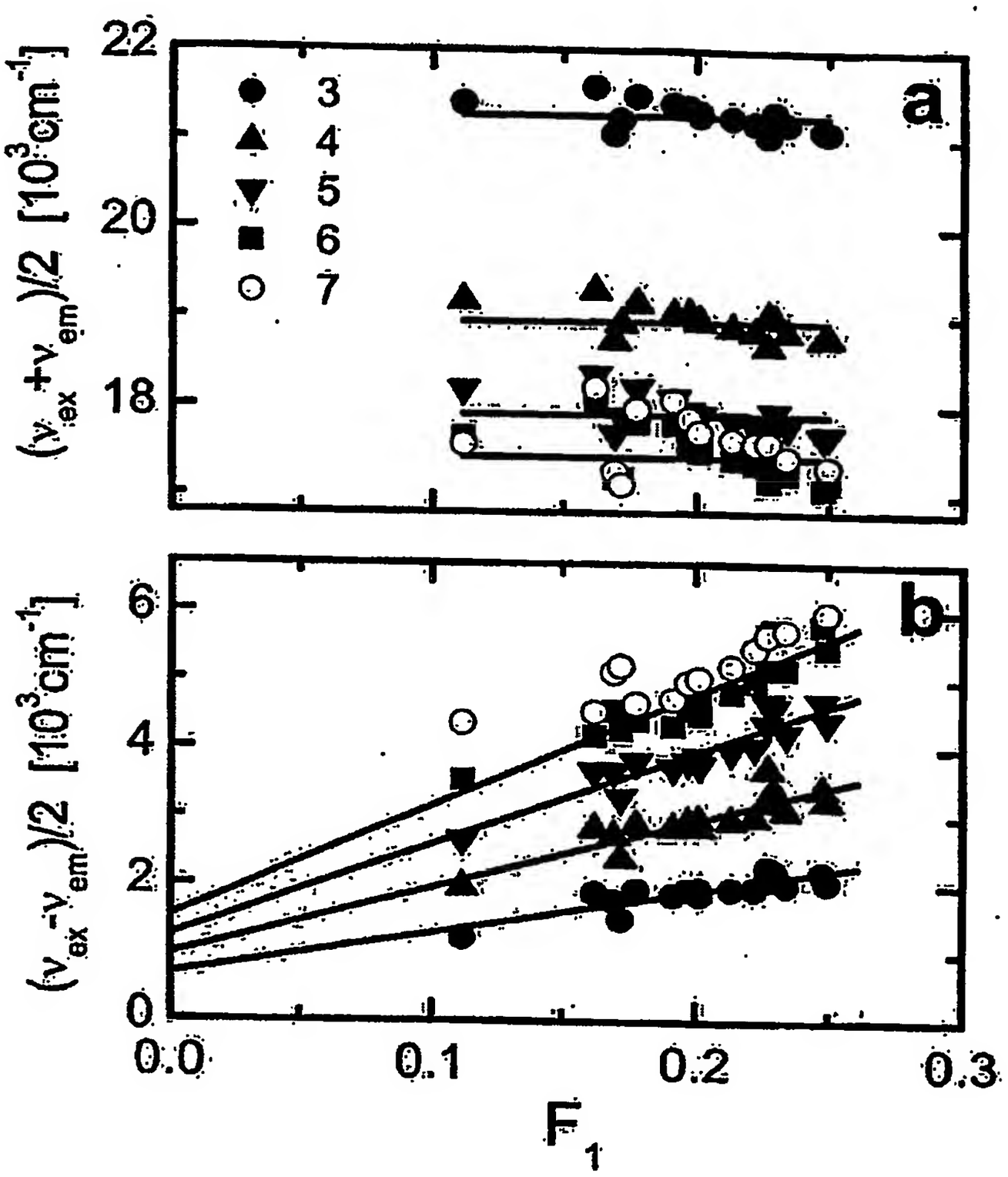

Fig. 4: Wavenumbers. Spectral features of ANNINE dyes in polar solvents. (a) Average $(\bar{\nu}_{ex}+\bar{\nu}_{em})/2$ of the spectral maxima of absorption and fluorescence versus polarity function F_1. The data are fitted with a constant wavenumber $\bar{\nu}_{00}$ for the 00 energy in vacuum. (b) Half of the Stokes shift $(\bar{\nu}_{ex}-\bar{\nu}_{em})/2$ versus polarity function F_1. The data of ANNINE-3 to ANNINE-6 are fitted with straight lines.

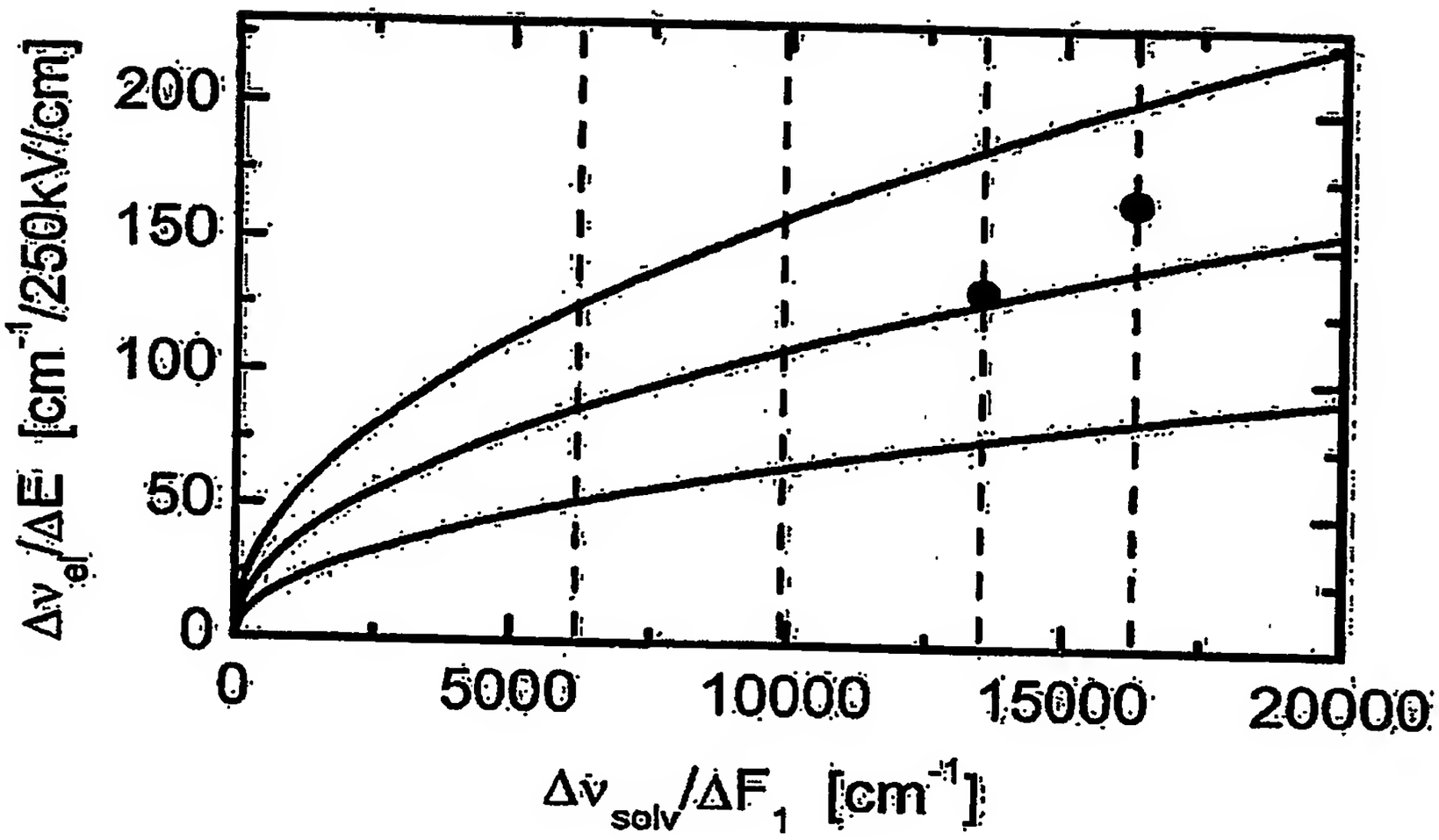

Fig. 5: Ordinate, abscissa, radius angeben. Relation of electrochromic spectral shift and solvatochromic sensitivity. The electrochromic shift $\Delta\bar{\nu}_{electro}$ expected for a voltage change of $\Delta V_M = 100mV$ across a membrane of thickness $d_M = 4nm$ is plotted versus the solvatochromic sensitivity $\Delta\bar{\nu}_{solv}$. The charge shift is assumed to be in the direction of the membrane normal with $\cos\vartheta = 1$. Three different radii of the effective radius a are considered. The experimental solvatochromic sensitivities of the ANNINE dyes are indicated by vertical lines. Two dots mark the experimental electrochromism of ANNINE-5 and ANNINE-6 in a neuron membrane.

10125

1 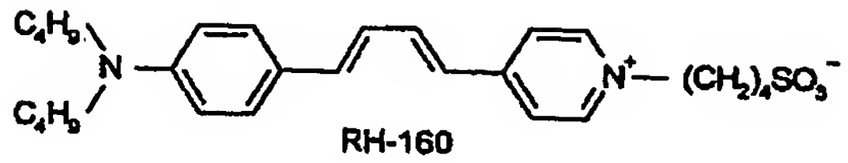

RH-160

2 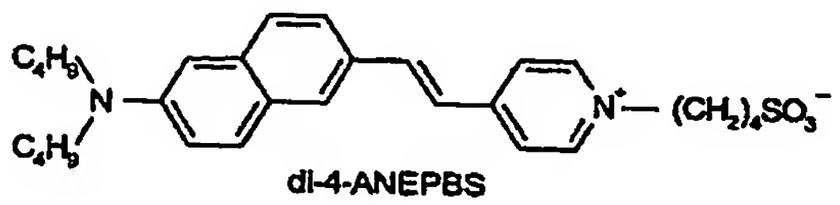

di-4-ANEPBS

3 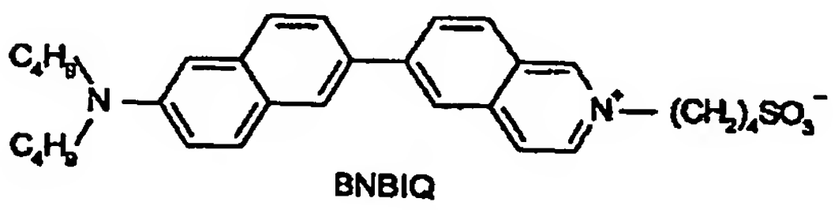

BNBIQ

4 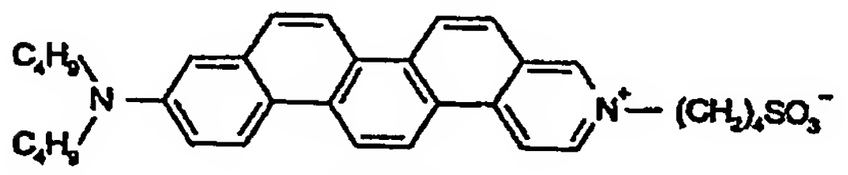

ANNINE-5

5 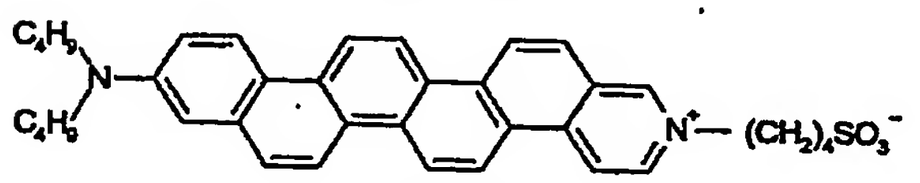

ANNINE-6

Figure 6 Voltage-sensitive amphiphilic hemicyanine dyes. (1)-(4) Homologous series with electron pushing aniline, electron pulling pyridinium and two intervening conjugated CC double bonds: styryl dye RH-160 (RH-421 with pentyl substitutents), styryl dye di-4-ANEBPS (di-4-ANEPPS with propylsulfonate), biaryl dye BNBIQ and anellated hemicyanine dye ANNINE-5. The conformation at the single bonds is matched to the structure of ANNINE-5. (5) Anellated hemicyanine dye ANNINE-6.

11.125.

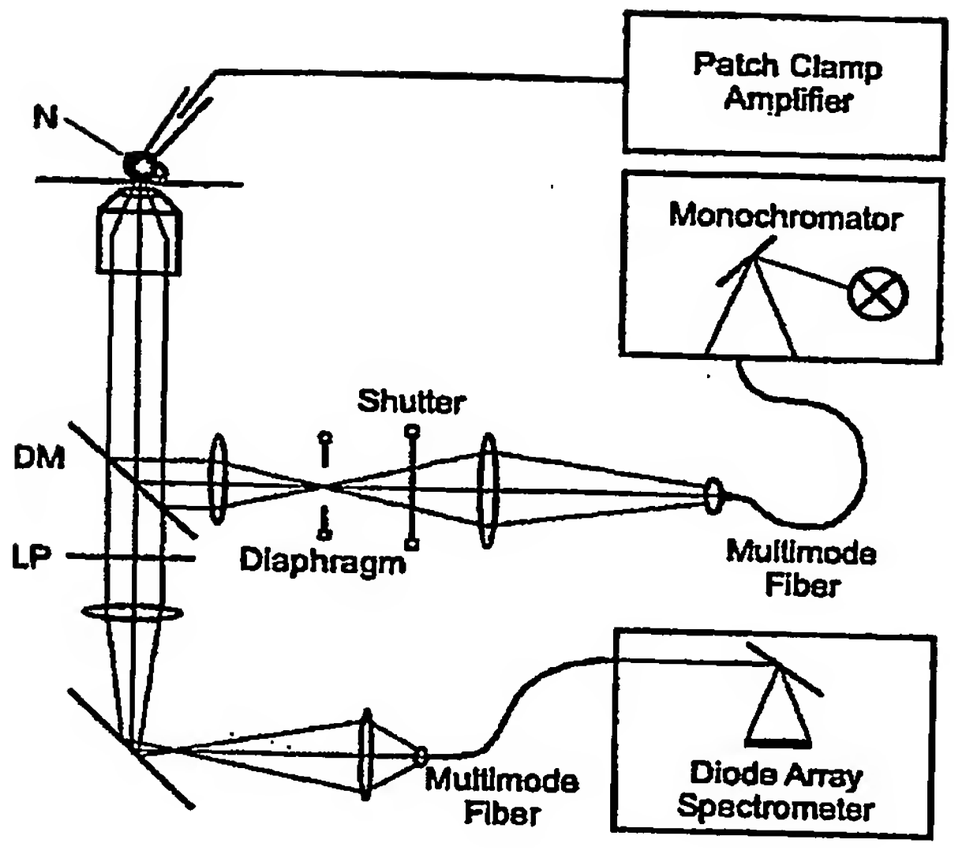

Figure 7 Experimental setup. A nerve cell (N) stained with a voltage sensitive dye is kept at a defined intracellular voltage by a micropipette using a patch-clamp amplifier. The cell is illuminated in a microscope through monochromator, shutter, dichroic mirror (DM) and objective. The fluorescence passes the dichroic mirror and a long pass filter (LP) and is detected by a diode array spectrometer. The complete fluorescence spectrum is recorded for a wide range of excitation wavelengths at two different transmembrane voltages.

12125

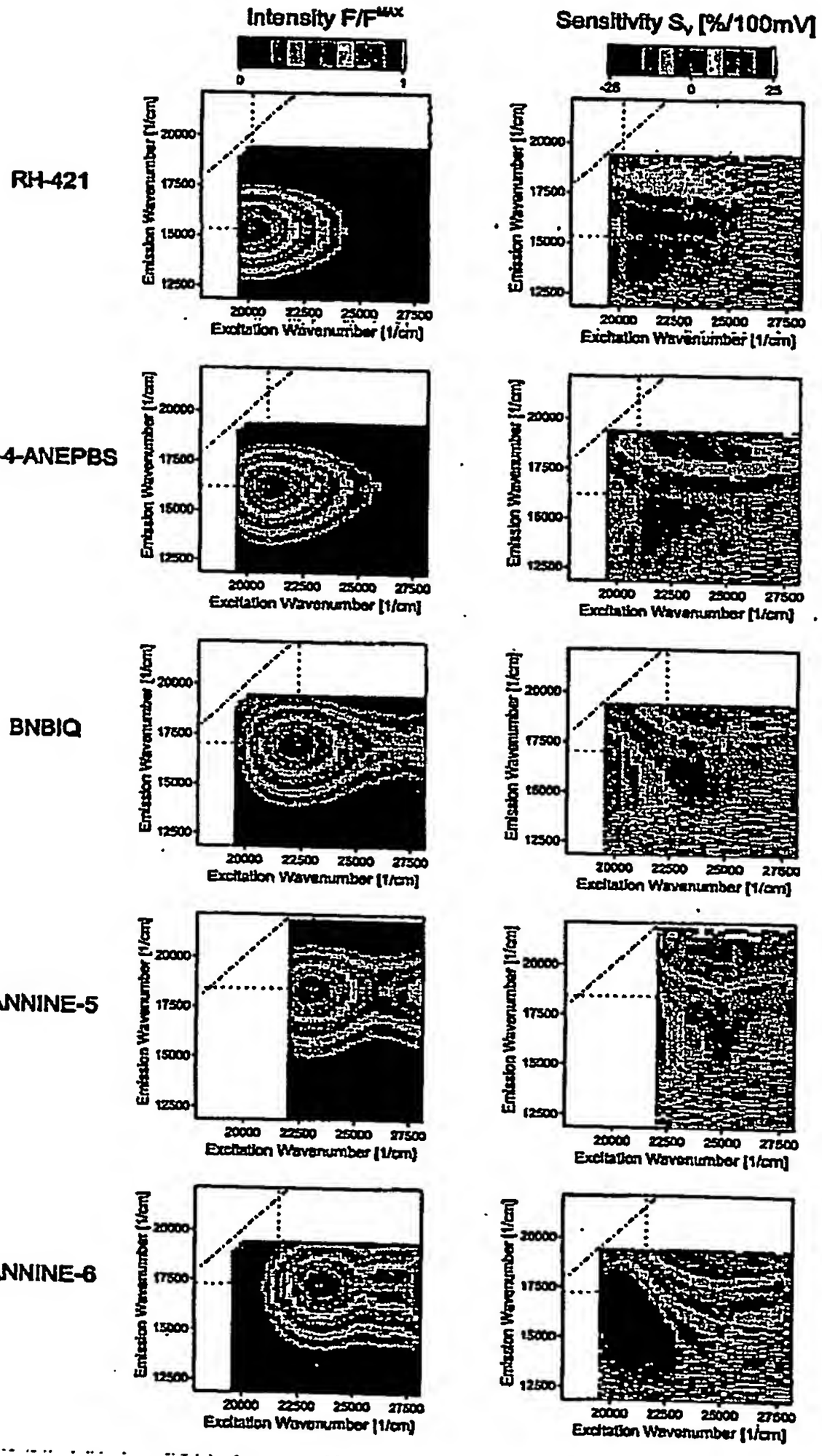

Figure 8. Experimental twodimensional fluorescence spectra. Left column: Color coded relative fluorescence intensity $F_V(\bar{\nu}_{ex},\bar{\nu}_{em})/F_V^{MAX}$ in Retzius cells at a voltage $V_M = -70mV$ as a function of the wavenumbers of excitation (abscissa) and emission (ordinate). Right column: Color coded voltage sensitivity of fluorescence $S_V(\bar{\nu}_{ex},\bar{\nu}_{em}) = \Delta F_V / F_V \Delta V_M$. The diagonal lines mark equal wavenumbers of excitation and emission. The dotted vertical and horizontal lines indicate onedimensional spectra of excitation and emission. They are chosen through the twodimensional maxima with the exception of ANNINE-6, where the excitation is chosen in the red to avoid a contribution of the S0/S2 transition.

13125

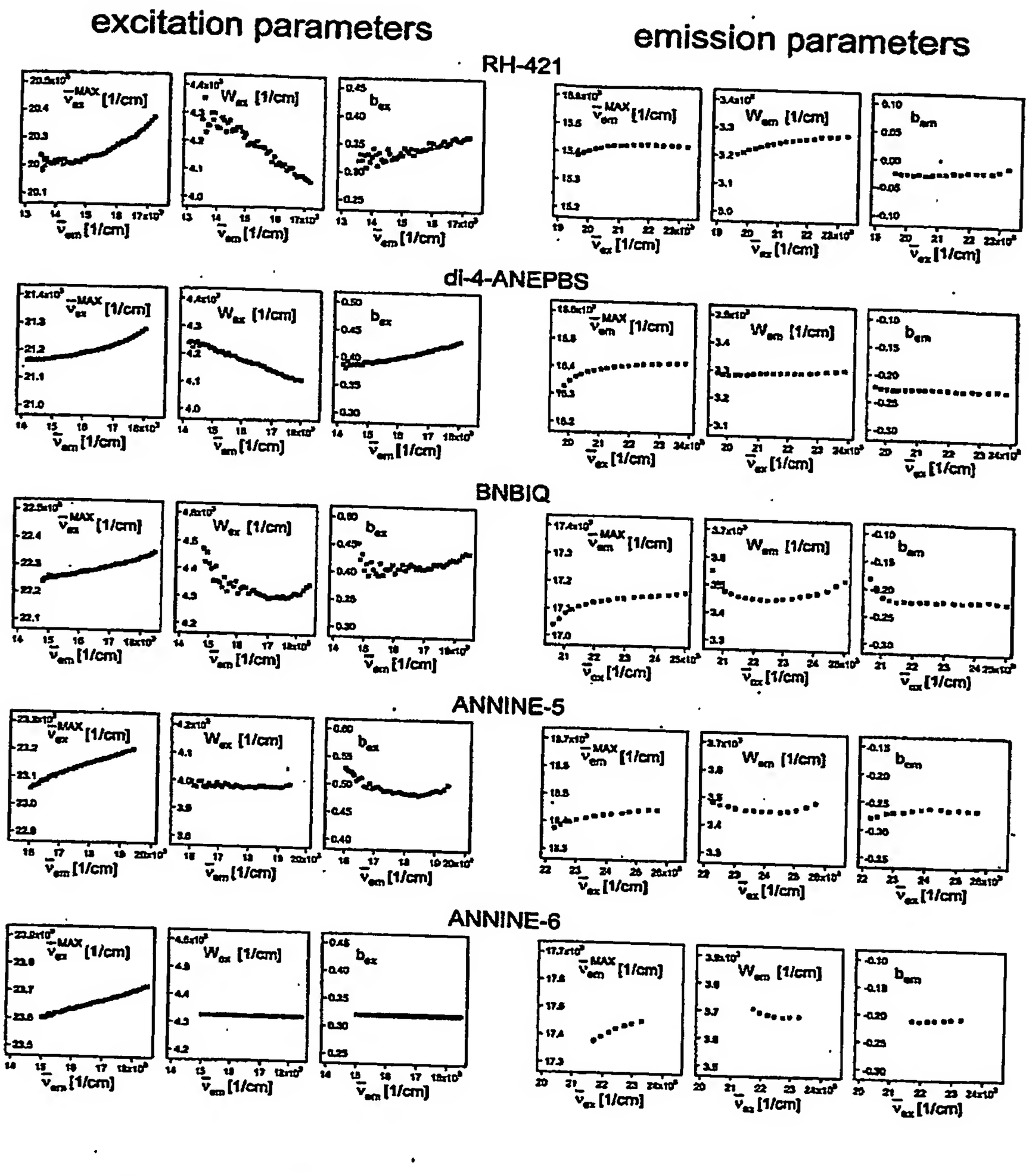

Figure 9 Mutual dependence of excitation and emission spectra. Left: Spectral parameters of the excitation spectra (maximum $\bar{\nu}_{ex}^{MAX}$, width W_{ex}, asymmetry b_{ex}) as a function of the emission wavenumber $\bar{\nu}_{em}$. Right: Spectral parameters of the emission spectra (maximum $\bar{\nu}_{em}^{MAX}$, width W_{em}, asymmetry b_{em}) as a function of the excitation wavenumber $\bar{\nu}_{ex}$.

14125

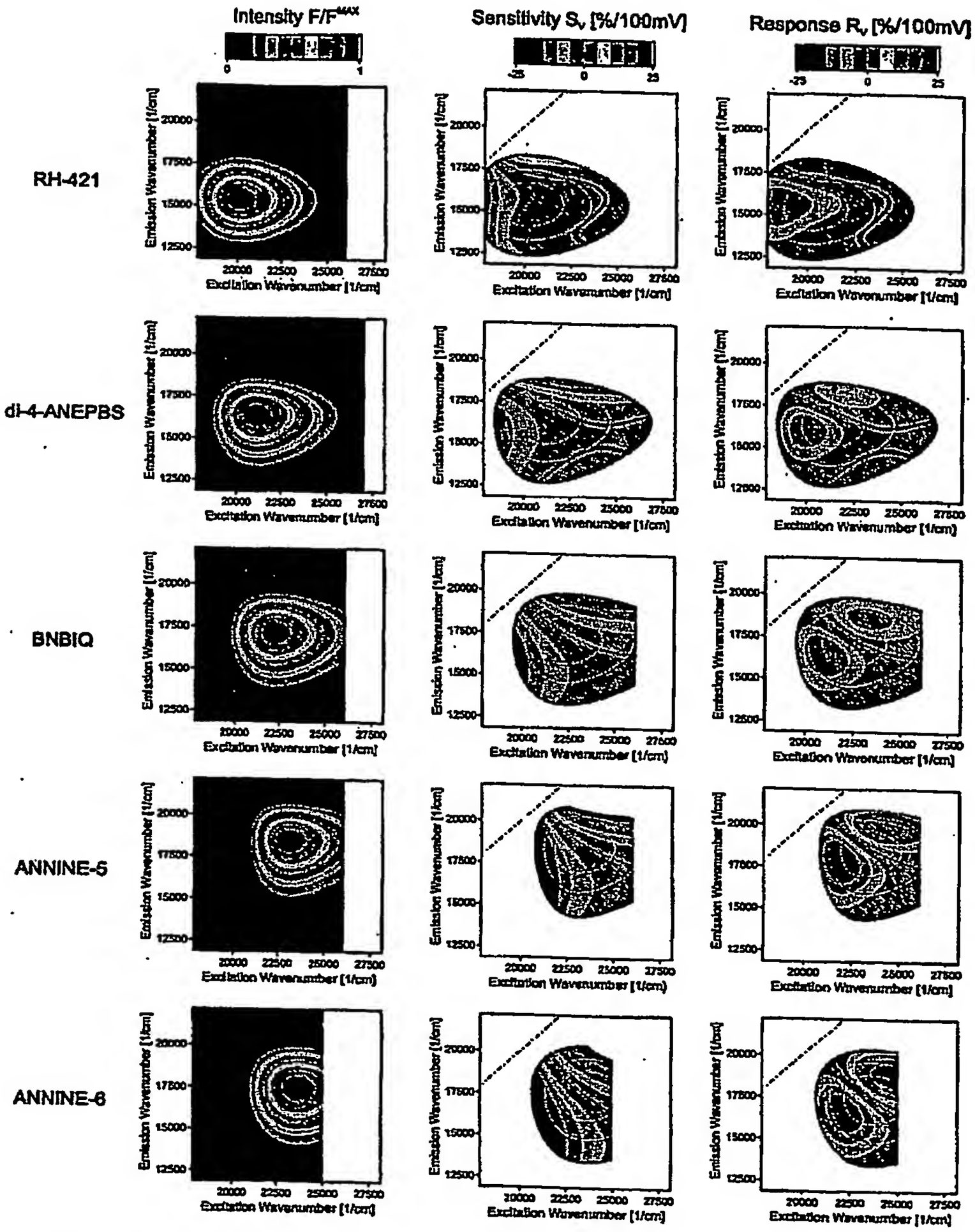

Figure 10 Twodimensional fluorescence spectra parametrized by a product of lognormal functions. Left column: color coded relative fluorescence spectra $F_{\bar{\nu}}(\bar{\nu}_{ex},\bar{\nu}_{em})/F_{\bar{\nu}}^{MAX}$ at $V_M = -70mV$. Central column: color coded sensitivity spectra $S_V(\bar{\nu}_{ex},\bar{\nu}_{em}) = \Delta F_{\bar{\nu}}/F_{\bar{\nu}}\Delta V_M$ in a range where $F_{\bar{\nu}}/F_{\bar{\nu}}^{MAX} > 0.1$ and where the S_0/S_2 transition plays a negligible role. Right column: color coded relative response spectra $R_V = \Delta F_{\bar{\nu}}/F_{\bar{\nu}}^{MAX}\Delta V_M$. The diagonals mark equal wavenumbers of excitation and emission. White lines in the sensitivity and response spectra indicate the intensity levels $F_{\bar{\nu}}/F_{\bar{\nu}}^{MAX} = 0.33$ and $F_{\bar{\nu}}/F_{\bar{\nu}}^{MAX} = 0.67$. Black lines mark the change of sign in sensitivity and response.

15125

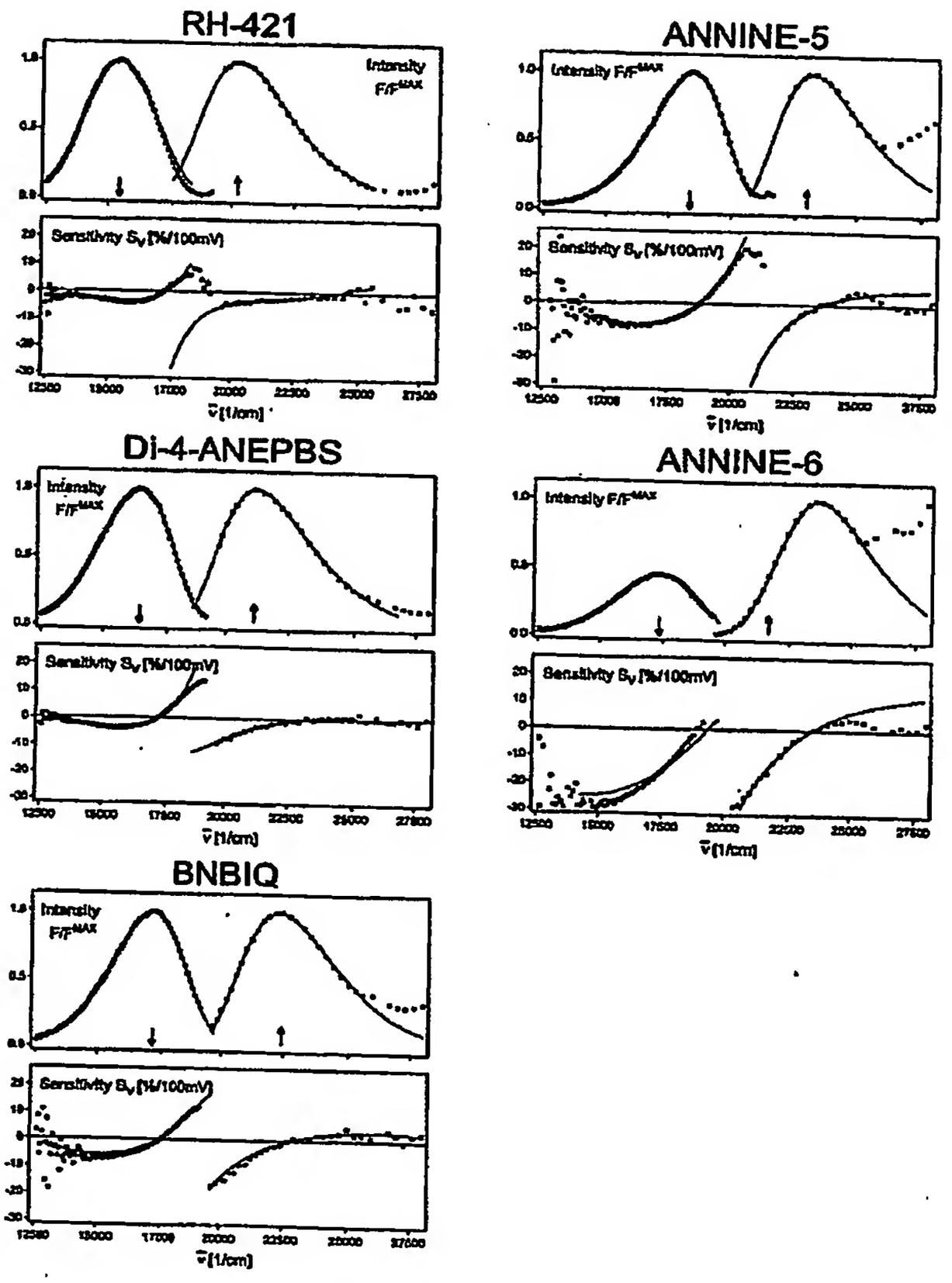

Figure 11 Onedimensional spectra of fluorescence and voltage sensitivity. Upper plots: spectra of relative intensity of emission $F_V(\bar{\nu}_{em})/F_V^{MAX}$ and of excitation $F_V(\bar{\nu}_{ex})/F_V^{MAX}$ across the twodimensional spectra as indicated in Fig. 3. Lower plots: sensitivity spectra of emission $S_V(\bar{\nu}_{em})$ and of excitation $S_V(\bar{\nu}_{ex})$. The drawn lines are onedimensional sections of the fit with a product of two lognormal functions taken from Fig. 5. The wavenumbers of excitation and emission are marked by arrows.

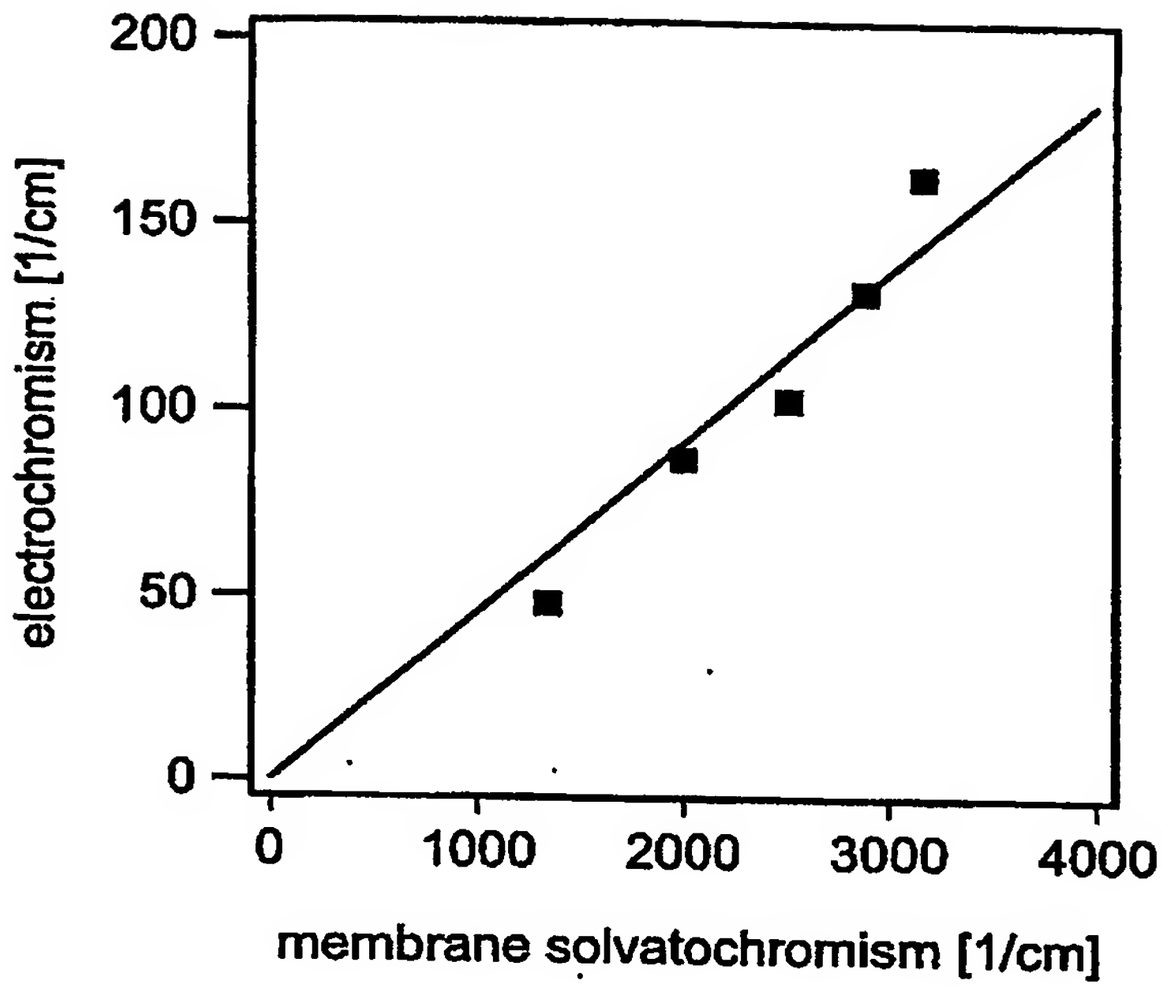

Fig.12 Electrochromism and membrane solvatochromism. Blue shift $\Delta\bar{\nu}_{ex}^{MAX}$ of the excitation spectra induced by a membrane voltage of $\Delta V_M = 100mV$ versus shift $\Delta\bar{\nu}_{00} = \bar{\nu}_{00}^{mem} - \bar{\nu}_{00}$ of the average wavenumber of excitation and emission $\bar{\nu}_{00}^{mem} = \left(\bar{\nu}_{ex}^{MAX} - \bar{\nu}_{em}^{MAX}\right)/2$ in the membrane with respect to the 00 energy $\bar{\nu}_{00}$ in bulk solvents. The dots refer to the dyes 1-5 in Fig. 1. The linear regression line has a slope of 0.045.

17125

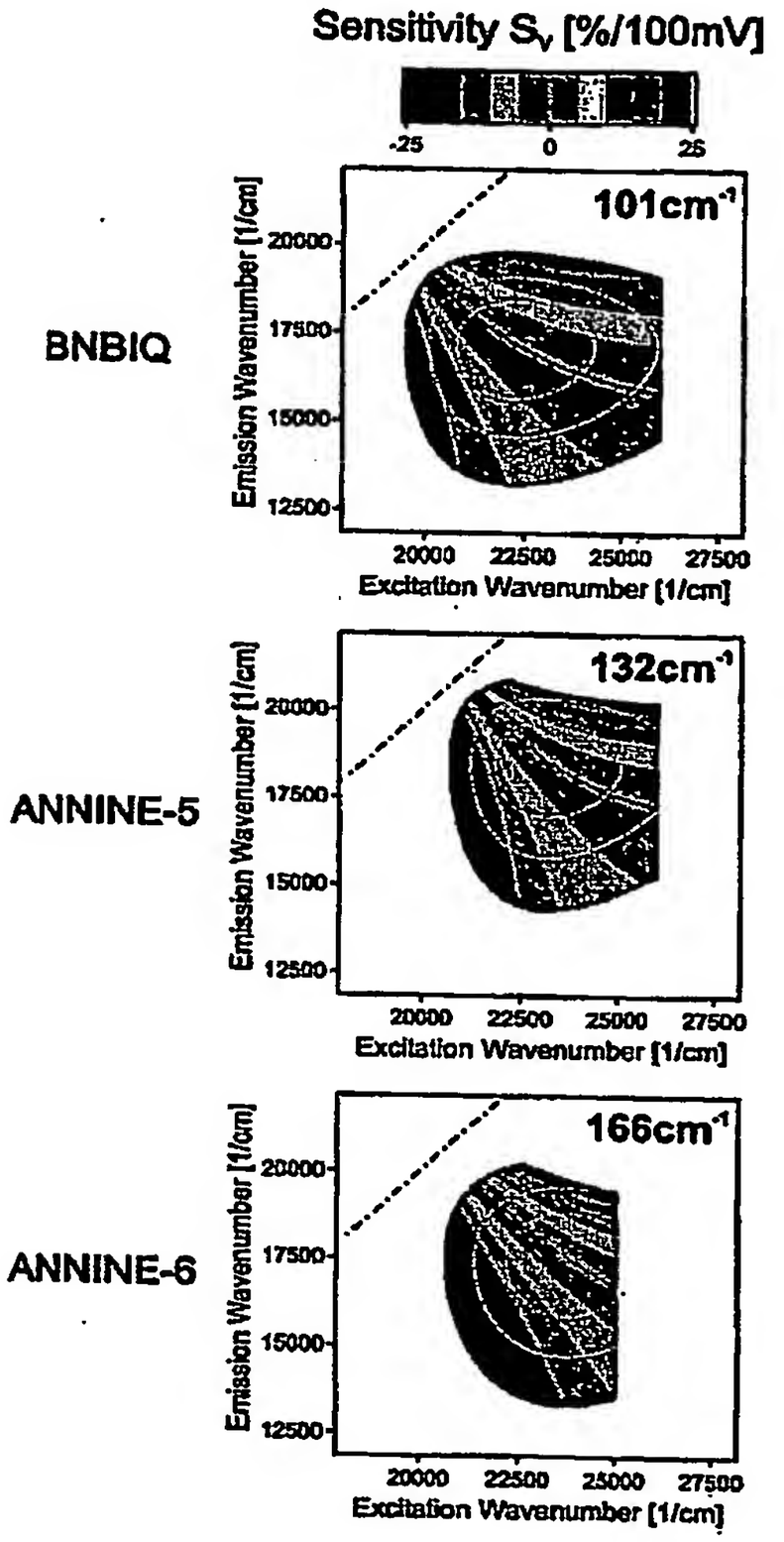

Figure 13 Voltage sensitivity for molecular Stark effect. Color coded sensitivity spectra $S_V(\bar{\nu}_{ex},\bar{\nu}_{em}) = \Delta F_V / F_V \Delta V_M$ in a range of relative intensity $F_{\bar{\nu}}/F_{\bar{\nu}}^{MAX} > 0.1$ where the S_0/S_2 transition plays a negligible role. The spectral shifts of excitation and of emission by a voltage change of $\Delta V_M = 100mV$ are $\Delta\bar{\nu}_{ex,em} = 101cm^{-1}$ for BNBIQ, $\Delta\bar{\nu}_{ex,em} = 132cm^{-1}$ for ANNINE-5 and $\Delta\bar{\nu}_{ex,em} = 166cm^{-1}$ for ANNINE-6. The diagonals mark equal wavenumbers of excitation and emission. White lines in the sensitivity and response spectra indicate the intensity levels $F_{\bar{\nu}}/F_{\bar{\nu}}^{MAX} = 0.33$ and $F_{\bar{\nu}}/F_{\bar{\nu}}^{MAX} = 0.67$. Black lines mark the change of sign in sensitivity and response.

18125

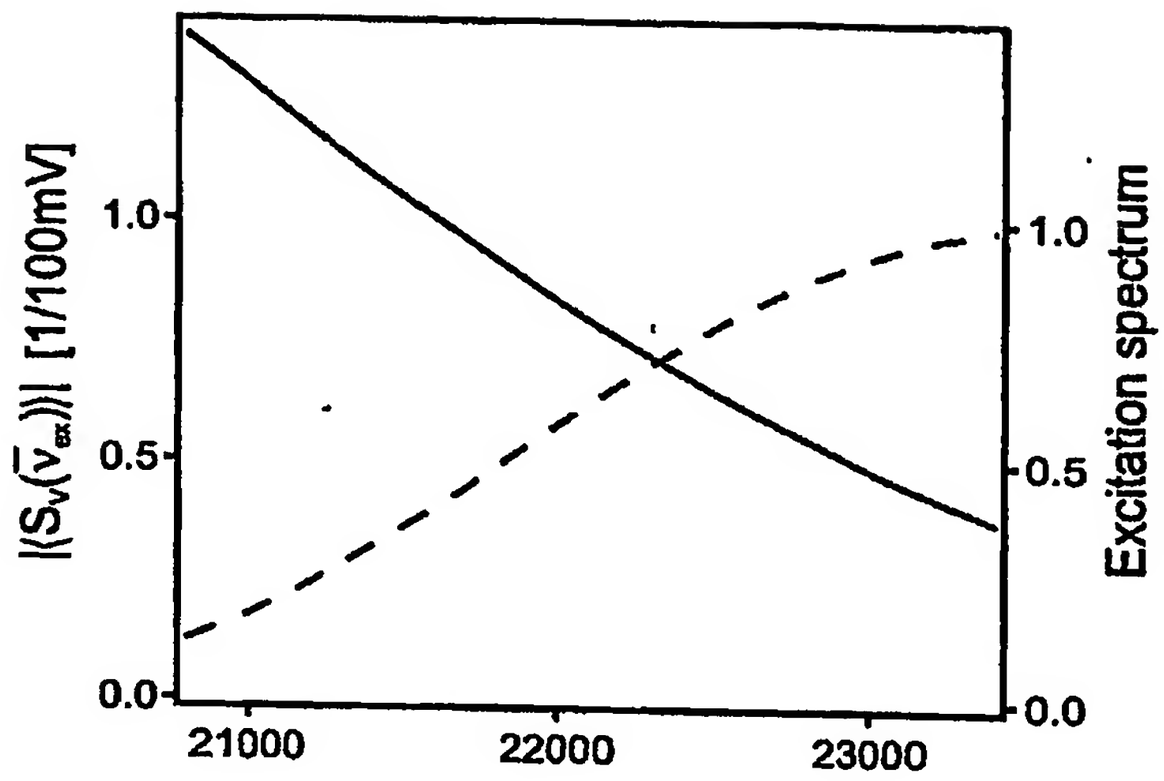

Figure 14 Weighted voltage sensitivity $|\langle S_V(\bar{\nu}_{ex})\rangle|$ of ANNINE-6 versus wavenumber of monochromatic excitation (full line) $\bar{\nu}_{ex}$. $|\langle S_V(\bar{\nu}_{ex})\rangle|$ is proportional to the signal-to-noise ratio with the constraint of a constant number of excitation processes per unit time. The detection ranges from $12000 cm^{-1}$ to $17600 cm^{-1}$. For comparison the relative excitation spectrum is plotted (dashed line).

19125

(a)

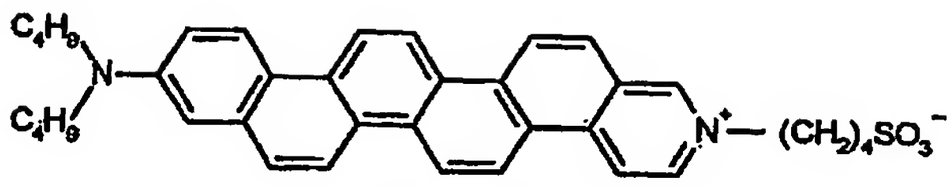

ANNINE-6

(b)

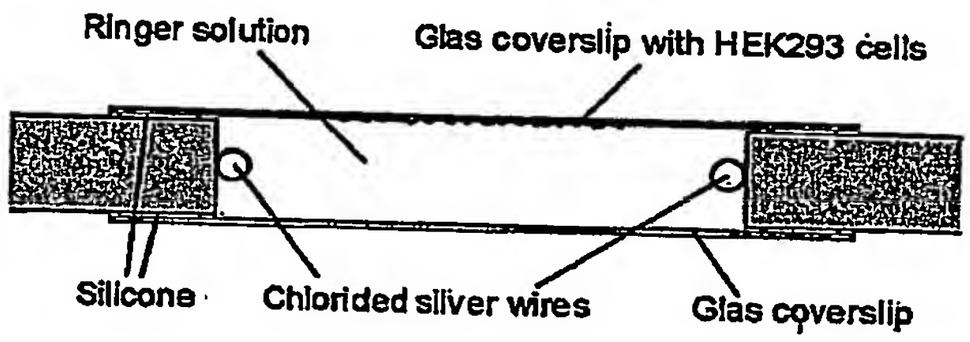

Fig.15 Structure of the new voltage-sensitive dye ANNINE-6 (a). Electric field application chamber (b). Cells are not drawn to scale. The Ringer flowes perpendicular to the paper plain.

20125

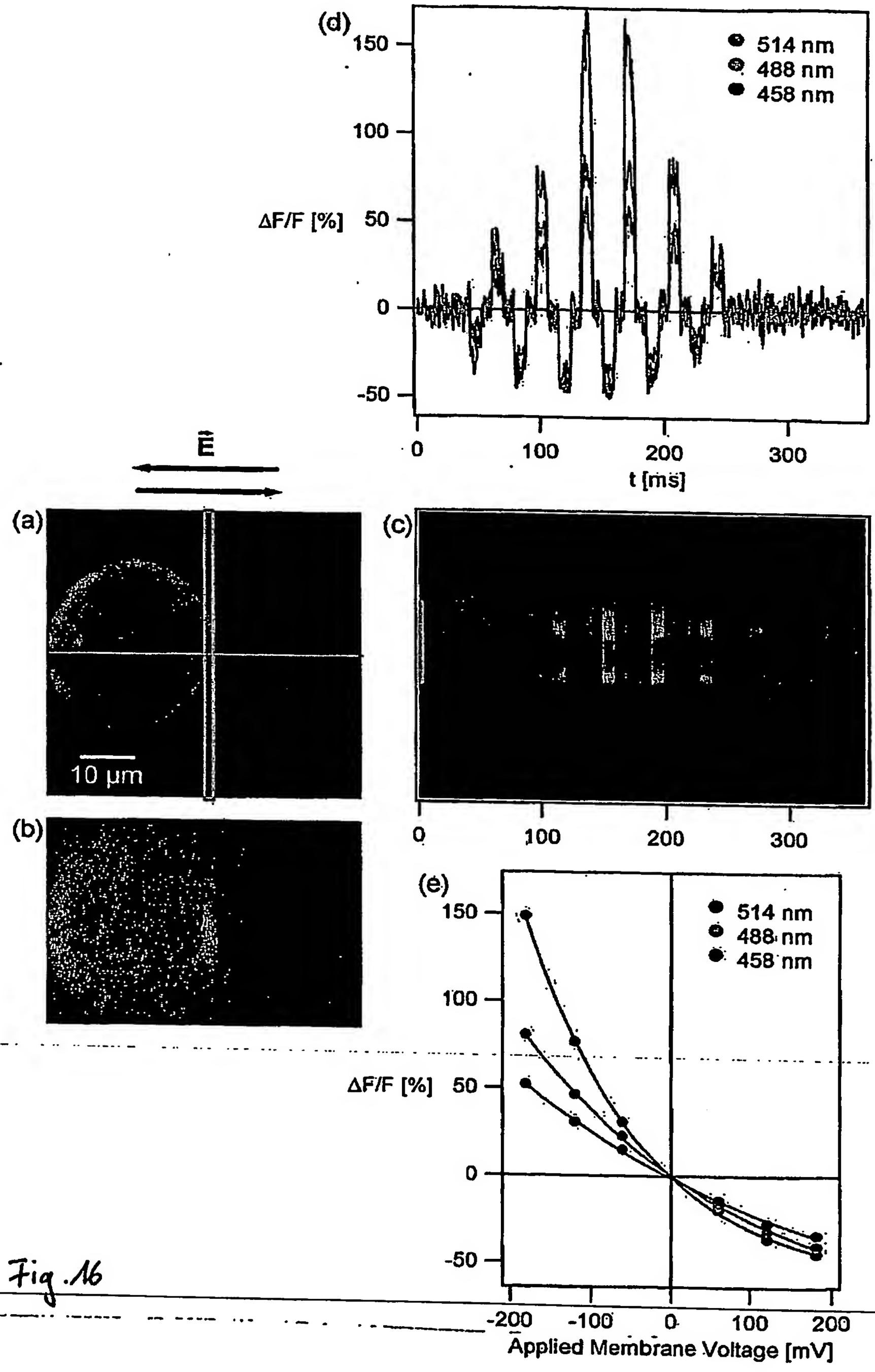
(d)
150
100
50
0
-50
ΔF/F [%]
514 nm
488 nm
458 nm
0
100
200
300
t [ms]
Ē
(a)
10 µm
(b)
(c)
0
100
200
300
(e)
150
100
50
0
-50
ΔF/F [%]
514 nm
488 nm
458 nm
-200
-100
0
100
200
Applied Membrane Voltage [mV]

Fig. 16

Fig.16 Voltage-sensitive dye signals from HEK293 cells stimulated by external electric fields. Fluorescence is excited by an Ar-ion laser. XY scan (a) and XZ scan (b) at the horizontal line marked in (a) of a cell stained with ANNINE-6 show the high membrane affinity of the amphiphilic dye. The open box in (a) markes the position of the line scan (c). Here it was scanned perpendicular to the external electric field. The line scan was aquired at an excitation wavelength of $514\ nm$ and is the average of 12 measurements. The relative fluorescence changes increase when the excitation wavelength is increased from $458\ nm$ over $488\ nm$ to $514\ nm$ (d). The $514\ nm$ time trace is the average of the in (c) marked traces. The relative fluorescence changes of (d) over the applied membrane voltage is not linear but fits to an exponential curve (e). For the calculation of the applied membrane voltage only the diameter and not the shape of the cell was considered.

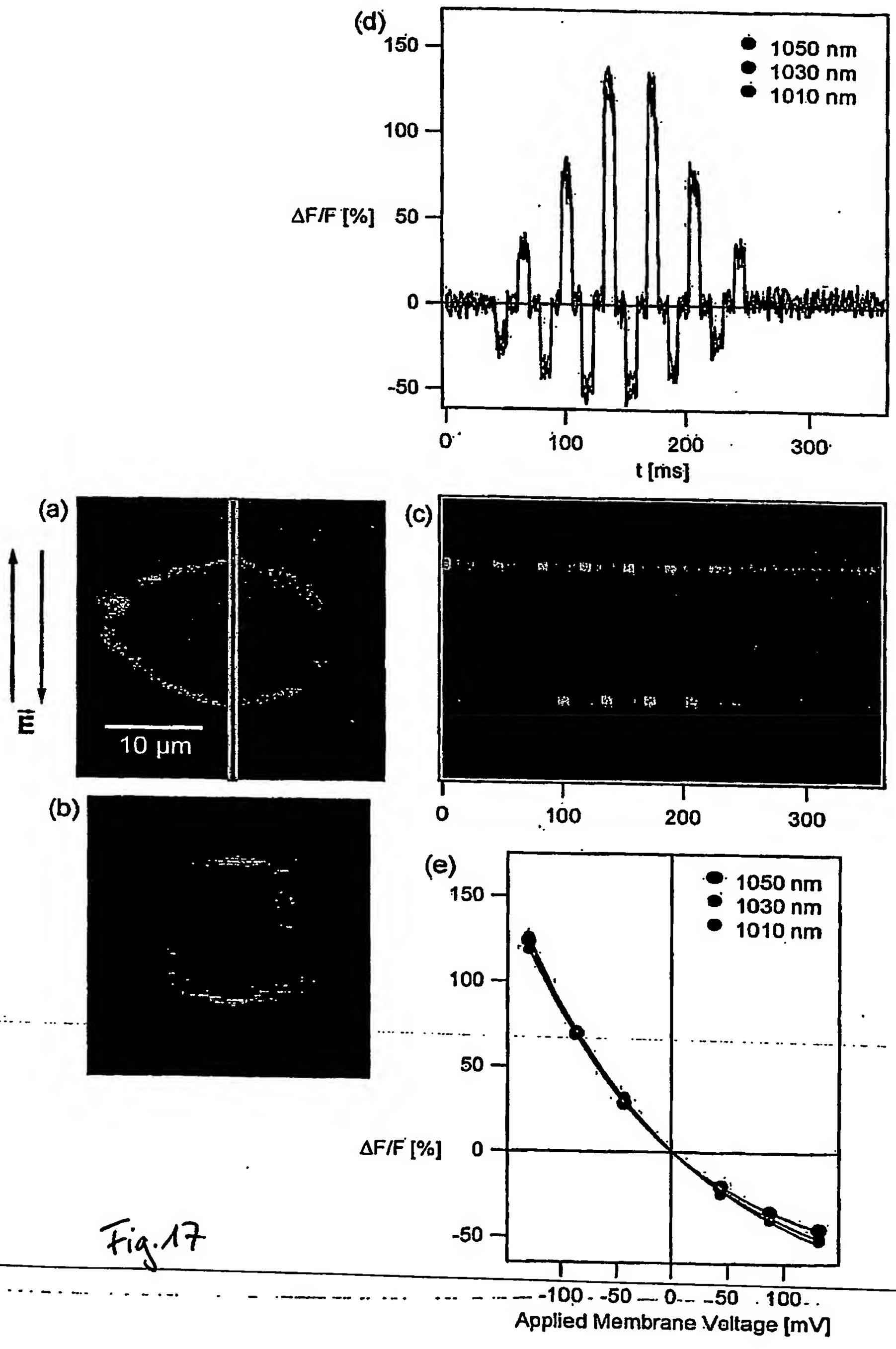
(d)
1050 nm
1030 nm
1010 nm
150
100
50
0
-50
ΔF/F [%]
0
100
200
300
t [ms]
(a)
E
10 µm
(b)
(c)
0
100
200
300
(e)
1050 nm
1030 nm
1010 nm
150
100
50
0
-50
ΔF/F [%]
-100
-50
0
50
100
Applied Membrane Voltage [mV]

Fig.17

Fig. 7 Voltage-sensitive dye signals from HEK293 cells with two-photon excitation stimulated by external electric fields. XY scan (a) and YZ scan (b) at the vertical open box marked in (a) of a cell stained with ANNINE-6. The open box in (a) also markes the position of the line scan (c). In this case we scanned parallel to the external electric field. Note the reverse fluorescence change in the opposite membran areas. The line scan was aquired at an excitation wavelength of $1050\ nm$ and is the average of 12 measurements. The relative fluorescence changes is rather the same at $1010\ nm$, $1030\ nm$ and $1050\ nm$ excitation (d). The $1050\ nm$ time trace is the average of the in (c) marked traces. The relative fluorescence changes of (d) over the applied membrane voltage is fitted by an exponential curve (e). For the calculation of the applied membrane voltage only the diameter and not the shape of the cell was considered.

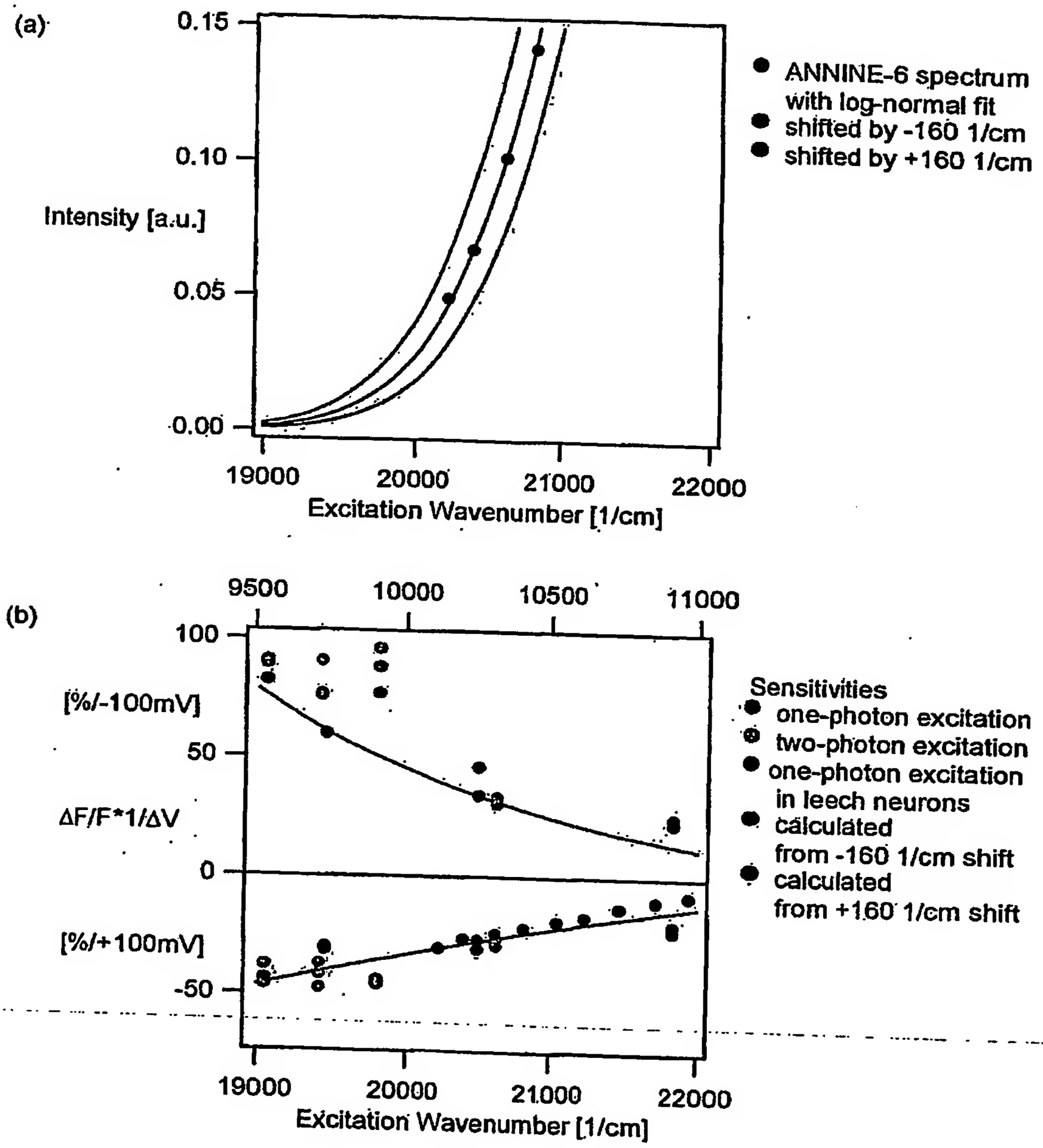
(a)
0.15
0.10
0.05
0.00
Intensity [a.u.]
19000
20000
21000
22000
Excitation Wavenumber [1/cm]
ANNINE-6 spectrum with log-normal fit
shifted by -160 1/cm
shifted by +160 1/cm
(b)
9500
10000
10500
11000
100
50
0
-50
[%/-100mV]
ΔF/F*1/ΔV
[%/+100mV]
19000
20000
21000
22000
Excitation Wavenumber [1/cm]
Sensitivities
one-photon excitation
two-photon excitation
one-photon excitation in leech neurons
calculated from -160 1/cm shift
calculated from +160 1/cm shift

Fig. 18

Fig.18 Spectrum and sensitivity of ANNINE-6 at the red edge of the excitation. The spectrum of ANNINE-6 in a leech neuron (Kuhn & Fromherz) is fitted with a log-normal function and interpolated (a). A pure Stark effect leeds to a spectral shift of -/+160 1/cm (Kuhn & Fromherz) for an extracellular stained cell and a voltage change in the cell of -/+100mV (blue, green). The resulting relative fluorescence change is shown in (b). Sensitivity measurements in leech neurons of a depolarization fit pretty well (black). Also the relative fluorescence change per $\pm 100\ mV$ are shown at different one-photon and two-photon excitation wavelength in HEK293 cells. The values were taken from exponential fits (e.g. Fig.2e, 3e). Measurements of 6 cells account for the diagramm.